Science of the Total Environment 874 (2023) 162476

Contents lists available at ScienceDirect

Science of the Total Environment

journal homepage: www.elsevier.com/locate/scitotenv

Comparing the cooling effectiveness of operationalisable urban surface combination scenarios for summer heat mitigation

Prabhasri Herath [a], Marcus Thatcher [b], Huidong Jin [c], Xuemei Bai [a,*]

[a] Fenner School of Environment and Society, Australian National University, Canberra, Australia
[b] CSIRO Marine and Atmospheric Research, Aspendale, Victoria, Australia
[c] CSIRO Data61, GPO Box 1700, Canberra, ACT 2601, Australia

HIGHLIGHTS

- 18 scenarios were simulated over 10 years to determine the cooling effectiveness in Melbourne.
- Different urban surface parameters: vegetation cover, green & cool roof levels were used.
- Effectiveness of scenarios needs to be defined with both thermal and operational factors.
- Higher reductions observed for average & extreme summer heat with combined parameters.
- Hence, combined scenarios were found to be the most effective and operationalisable.

GRAPHICAL ABSTRACT

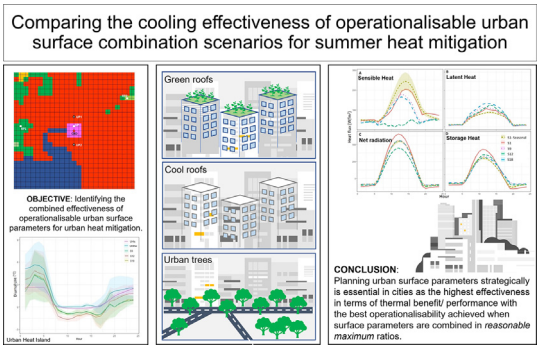

ARTICLE INFO

Editor: Martin Drews

Keywords:
Heatwaves
Green roofs
Cool roofs
Urban surface parameters
Heat reduction
Effectiveness

ABSTRACT

Extreme summer heat in cities exacerbates the vulnerability of urban communities to heatwaves. Vegetative and reflective urban surfaces can help reduce urban heat. This study investigated the impacts of urban trees, green roofs and cool roofs on heat mitigation during average and extreme summer conditions in temperate oceanic Melbourne, Australia. We simulated the city climate using 'The Air Pollution Model' (TAPM) at a 1 km spatial resolution over 10 years, which according to our review of the literature, was the most prolonged period for simulation in Melbourne. During a widespread heatwave event, some of the tested scenarios with combined surface parameters could reduce the extreme values of the energy budget components- sensible heat, latent heat, and storage heat fluxes up to seasonal averages compared to the existing situation for Melbourne (control). The scenario with the highest (reasonable maximum) ground-level vegetation, green roofs, and cool roofs could reduce air temperatures up to 2.4 °C. The simulations suggest that a combined strategy with vegetative and high-albedo surfaces will deliver higher effectiveness with maximum cooling benefits and cost-effectiveness than individual strategies in cities. These results suggest the importance of collaborative strategic planning of urban surfaces to make cities healthier, sustainable, and liveable.

1. Introduction

A high concentration of population and urban functions intensifies the consequences of extreme heat in cities (Fischer et al., 2012). Heatwaves are critical extreme heat events in cities that directly affect the thermal comfort of city occupants while overloading every sector, such as energy, health, economy, environment, and critical social infrastructure (WHO,

* Corresponding author.
E-mail addresses: Prabhasri.Herath@anu.edu.au (P. Herath), marcus.thatcher@csiro.au (M. Thatcher), warren.jin@data61.csiro.au (H. Jin), xuemei.bai@anu.edu.au (X. Bai).

http://dx.doi.org/10.1016/j.scitotenv.2023.162476
Received 3 March 2022; Received in revised form 17 February 2023; Accepted 21 February 2023
Available online 28 February 2023

2018a; WHO, 2018b; AECOM, 2012; Hou et al., 2014; Ali et al., 2013; Wondmagegn et al., 2021). Extreme heat events persist for three or more consecutive days with high and unusual maximum and minimum temperatures at a particular location are defined as heatwaves (BoM, 2016). They are meteorological events driven by a persistent high-pressure system coupled with low soil moisture on the land surface (dominant sensible heat fluxes over latent in dry soil) (Perkins, 2015). Climate change has increased the likelihood and severity of heatwaves worldwide (Schiermeier, 2019; Phillips, 2020; Schiermeier, 2021; Coutts et al., 2007). Melbourne's maximum and minimum temperatures reached 45.1 °C and 25.7 °C, respectively, during the 2009- South-eastern Australian heatwave (VAGO, 2014). The health impacts of heatwaves are magnifying with increased maximum temperature during the day and more pronounced at night with elevated minimum temperatures (Williams et al., 2012). Urban Heat Island (UHI) effect is a microclimate phenomenon due to surface energy balance alterations, where near-surface air temperatures in cities are hotter than in adjacent non-urban areas (Roth, 2013). When UHI occurs during summer heatwaves (with low surface moisture and wind speeds (Li and Bou-Zeid, 2013), it can escalate the heatwave severity and increases health and human thermal comfort issues with intensified temperatures (Kueh et al., 2017). Therefore, investigating mitigation and adaptation strategies for extreme heat as well as UHI in cities is essential for a changing climate context.

Urban microclimate is determined by both natural and built environment-related (direct and indirect) factors. Natural factors range from latitude to elevation loss/gain, water bodies and natural land use, including wind direction and speed, air temperature, humidity, solar radiation, precipitation, soil type, greenery, to terrain conditions. The built environment factors include building materials, height, shape, colour, texture, urban green cover, canyons, built-up and open area ratio, anthropogenic water bodies and population density (Giyasova, 2021; Bherwani et al., 2020). Larger microclimates, such as cities, also reflect the influences back on temperature, wind, rainfall, snowfall, and air pressure (Shi et al., 2017; Patricola and Wehner, 2018; Rogers, 2018; Zhang et al., 2018). Inefficient evaporative cooling or reduced latent heat fluxes from insufficient green spaces and the aerodynamics of urban surface parameters cause changes in the energy budget that increase the surface temperature (Li et al., 2019; Zhao et al., 2014). Urban surface characteristics, such as vegetation cover, thermal properties of construction materials, density, form and fabric of buildings, city size, synoptic conditions, wind speed and flow, and anthropogenic heat, all act as drivers of UHIs (Oke et al., 1991; Zhou et al., 2017; Li et al., 2020).

Many studies have found a high correlation between urban heat and surface characteristics (Rogers, 2018; Zhang et al., 2018). Several strategic efforts on microclimatic heat mitigation via manipulating the above surface characteristics with urban planning and design measures have been highlighted in the literature. One example is applying engineering solutions with cool construction materials (low heat conductivity, low heat capacity, high solar reflectance and high permeability). This measure results in less heat absorption and storage during the day and subsequently low night heat emission. Another second example is using green infrastructure (GI) to reduce heat via evapotranspiration. Capturing solar energy for electricity generation, building underground, and leaving spaces between buildings are other proposed strategies in literature (Yenneti, 2020; Zeder, 2015; Yenneti et al., 2017). Retention of heat with water-sensitive urban designs is a useful mitigation strategy. Studies found water-sensitive urban designs can be useful as they hold and retain the excess heat. We found evidence that urban water bodies for reducing ambient air and land surface temperatures by 1–7 °C temperatures, depending on the season and the distance from the water body (Yenneti, 2020; Gupta et al., 2019; Jacobs et al., 2020). This is primarily due to the high heat capacity and evaporative cooling of water bodies. However, Theeuwes et al. showed that increased humidity during evaporation from waterbodies (when the water is warmer than the air temperature) may limit the cooling and thermal comfort or even increase the air temperature (Theeuwes et al., 2013). It has been demonstrated that individual independent design strategies are effective for different regions and climate zones (Jamei et al., 2021). Given that roofs and pavements (impervious surfaces) can cover around 60–90 % of urban surfaces in an urban area (Akbari et al., 2009; Stewart and Oke, 2012), changing their surface characteristics (e.g., increase surface albedos to reflect more light or enhance evaporative cooling using cool roofs and green roofs) could be a highly viable, effective option (Herath et al., 2021; Zinzi and Agnoli, 2012; Xing and Jones, 2019; Morini et al., 2018; Oswald et al., 2020; Herath et al., 2018a; Imran et al., 2018). Moreover, promoting vegetative surfaces by increasing street trees, urban parks, and other green spaces generally lowers the temperature by evapotranspiration and shade (Li and Norford, 2016; Imran et al., 2019a; Bowler et al., 2010; Richards et al., 2019), and also limits with some conditions such as irrigation and changes in urban aerodynamics with overcrowded urban trees (Heusinger et al., 2018; Park et al., 2019; Meili et al., 2021). Therefore, heat mitigation strategies for cities should be comprehensively planned and investigated to achieve expected outcomes.

In Australia, the death toll from heatwaves has exceeded that of any other natural environmental disaster (including bushfires, floods and cyclones) (DEA, 2020). Over 36,000 deaths were recorded associated with heat during 2006–2017, which was 2 % of total deaths in Australia (Longden et al., 2020). Some modelling results predict that future extreme heat events will increase in severity, duration, and frequency (Cowan et al., 2014). The occurrence of heatwaves in Melbourne, for example, has been frequent for the last two decades (Perkins-Kirkpatrick et al., 2016). Melbourne experienced a deadly, record-breaking heatwave in the summer of 2009, followed by another in 2014. With 1.52 °C above-average temperatures, 2019 was reported as the warmest year on record (BoM, 2020b). Several modelling studies on Australia have been conducted to find feasible mitigation strategies that minimise excessive heat. However, most studies have a limited scope because they consider a single event (either heatwaves or UHI) or a limited period of a single year (Zeder, 2015), except for Imran et al. (Imran et al., 2019b). Most studies on Melbourne have focused on the heatwaves in 2009, 2012, or 2014 (AECOM, 2012; Cowan et al., 2014; Morris et al., 2001). Jacobs et al. found a non-synergistic relationship between the cooling effect and the combined scenarios in an analysis focused on cool roofs and urban vegetation, using the Weather Research and Forecasting Model (WRF) in Melbourne (Jacobs et al., 2018). Chapman et al. performed a multi-year study by using the Conformal Cubic Atmospheric Model (CCAM) with urban vegetation and building density for Brisbane (Chapman et al., 2018) and found that vegetation cover had a more substantial impact on temperature than the building height and aspect ratio. Studies have also shown a significant increase in future nighttime UHIs with urban growth. For example, using The Air Pollution Model (TAPM), Coutts et al. showed nighttime UHI intensity would increase by 2030 with growing urban density (Coutts et al., 2008), and Imran et al. showed an increase in UHI in the range of 0.75–5.4 °C over the modelling area during the night, with predicted urban expansion by 2050 (Imran et al., 2019b).

The key objective of this study was to identify the combined effectiveness of different cooling strategies in terms of operationalisability for urban heat mitigation, using Melbourne as a case study. Since each city has a unique microclimate (Martilli et al., 2020; Masoudi et al., 2019), there are no one-size-fits-all planning solutions, and each city needs to identify their context-specific greening strategies for urban heat adaptation and mitigation. As one theory stated by Martilli et al. (Martilli et al., 2020), urban heat mitigation strategies do not define by the UHI intensity, and suggested as heat mitigation studies should shift beyond UHI mitigation to focus on the temperature difference between different urban areas instead of urban-rural based on recommendations of Stewart and Oke (2012). Therefore, this study presents empirical evidence in a mesoscale atmospheric model for Melbourne that tries a city-specific greening plan with operationalisable heat mitigation strategies which assessed with both urban-rural and urban-urban (between different Local Climate Zones-LCZs) gradients. The Melbourne metropolis was simulated in TAPM mesoscale atmospheric model to systematically investigate the combined impact of a mixed land use, land cover and surface properties: ground-level

vegetation, green roofs, and cool roofs on several heat-related indices. This was to assess the effectiveness of the combined surface parameters with their maximum heat reduction potential. For that, we investigated the diurnal thermal behaviour with air temperature and energy budget variations under different climatic conditions such as extreme and seasonal heat conditions. This study used 18 scenarios over 10 simulation years, a much larger sample size over a longer period than prior simulation studies. This approach was important for clarifying the combined impact of the different surface properties, as well as minimising the impact of year-to-year climate variability and improving the confidence interval, thereby providing more robust and rigorous results.

2. Methods

2.1. Study area

Melbourne covers 3770 ha and is the second-most populous city in Oceania. Approximately 854,000 people use the city daily, on average (City of Melbourne, 2017). Following the classification of LCZs (Stewart and Oke, 2012), Melbourne CBD represents a compact high-rise (LCZ1) build type while surrounding general urban areas exhibit compact low-rise (LCZ3) and open low-rise (LCZ6) with different land-use types (Fig. 1B). Melbourne has a temperate oceanic climate (Cfb) according to the Köppen climate classification. Melbourne's summer climate (December–February) is changeable with frequent hot and dry days with cold and wet spells, experiencing the highest mean monthly maximum temperature and an average 9 h duration of daily sunshine. The maximum (T_{max}) and minimum (T_{min}) temperatures ranged respectively from 24.2 to 26 °C and 13 to 14.6 °C (Site 086071), based on data from 1855 to 2015 (BoM, 2020a). Heat-related incidents, such as the UHI effect and heatwaves, are often observed in Melbourne. The highest summer T_{max} recorded was 46.4 °C on 7 February 2009 (Osmond et al., 2017). The Bureau of Meteorology (BoM) reported, on average, 30 days per year exceeding 30 °C (BoM, 2020a). The Melbourne UHI was recorded as 1.13 °C in 2001 (Morris et al., 2001); the central business district (CBD) reported 0.8 °C of UHI effect when non-CBD areas had a 30 °C day in 2012 (AECOM, 2012). UHI for land surface temperature varies from −7.16 to 10.2 °C in different metropolitan locations (Sun et al., 2019). These recent observations suggest that Melbourne might increase in density in terms of population and built-up areas in future and that the city should support this urban expansion while ensuring thermal comfort and liveability.

2.2. Model configuration

TAPM, developed by the Commonwealth Scientific and Industrial Research Organisation (CSIRO), Australia, was used in this study, and it dynamically downscales the three-dimensional meteorology and air pollution concentration to high spatial and temporal resolution over a small area (Hurley, 2008a). TAPM occupies an incompressible, non-hydrostatic, primitive equation model in its meteorological component, which supports the three-dimensional simulations with terrain-following vertical coordinates. A series of equations (momentum, incompressible continuity and scalar equations with turbulence kinetic energy and eddy dissipation rate) simulate different meteorological components, including horizontal and vertical wind flow and velocity, potential virtual temperature and specific humidity (Hurley, 2008b). In mesoscale modelling, urban parameterisations help to account for the area-average effect of urban interactions, including drag, turbulence production, heating, and the surface energy budget modification induced by buildings and urban land use (Brown, 2000). TAPM mesoscale modelling has also been coupled with the Urban Climate and Energy Model (UCLEM) to support this urban parameterisation, which is based on an urban canopy model (Thatcher and Hurley, 2012) and a building interior energy model (Lipson et al., 2018), intended to support multi-decade urban climate simulations in a computationally efficient way. Urban parameters in the simulations have been constrained to agree with available observations by Coutts et al. to provide the modelling process with as realistic and accurate parameters as possible for this location. The UCLEM is explicitly designed to represent the interactions between energy use and the urban environment in Australian cities over long time periods (e.g., decades). This model accommodates adjustments by the user for the parameters, including canyon and roof vegetation ratios, building height, density and the thermal and radiative characteristics of the building materials (Thatcher and Hurley, 2012; Lipson et al., 2018). As a result, it secures the mesoscale characterisations of urban surface parameters in large city-scale simulations.

The focus of this study was the urban canopy component of the model, where the canopy model supports 4 layers of building materials for road, roof and two walls, as well as an integrated canyon vegetation model and green roof parameterisation. Air circulation in the canyon for calculating

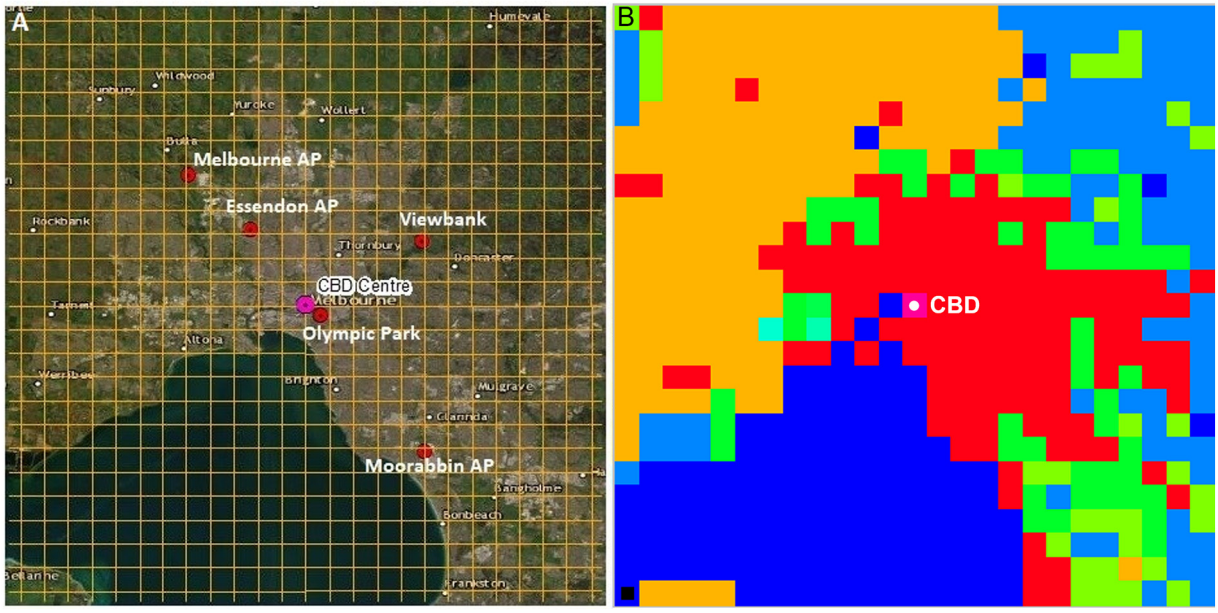

Fig. 1. Grid-level TAPM representation for the Melbourne CBD: A) ArcGIS image with 3 km grids developed for Melbourne with CBD centre and the weather stations used for model calibration, B) TAPM window of Melbourne with 3 km grid levels for different land uses (AP: airport).

turbulent fluxes is based on Harman et al. (Harman et al., 2004), which also facilitates the coupling of turbulent fluxes with the canyon vegetation. To improve the speed of the model over multi-decade timescales, the model employs a simplified big-leaf vegetation canopy parameterisation as well as tracking the vegetation water budget to a depth of 4 m, which provided a solution with reasonable accuracy for modelling latent heat flux despite the reduced number of prognostic variables (Thatcher and Hurley, 2012). The urban vegetation description is consistent with big-leaf canopy models used in climate land-surface models (Kowalczyk et al., 1994). The canyon floor is partitioned into vegetation and road areas, with separate albedo, roughness lengths and energy budget calculations. The canyon geometry is modified to account for changes in sky view factors (SVF) as well as accounting for canyon walls that are obscured by vegetation. This approach limits shading on the canyon floor to the vegetation tile, and there is no direct shading of the road 'tile' by the adjacent vegetation tile. Although there is an impact on the canyon floor due to the reflections of shortwave radiation between the walls, roads, vegetation, and the modified SVF.

Green roof vegetation is also based on a big-leaf canopy model, modifying the roof albedo and roughness length. The green roof water budget is also tracked, although the soil depth of the green roof is limited to 10 cm and thereby limits the maximum available water for evapotranspiration. A simple irrigation scheme was used where soil moisture was relaxed to a value of 75 % of the wilting value and 25 % of the saturated value over a 24-h period. Without irrigation parameterisation, the green roof typically dries out and becomes ineffective for reducing urban temperatures. Heat storage is represented by the roof, wall and road tiles, but not explicitly soil temperatures under the vegetation canopy, although the vegetation canopy has its own energy budget. This means that the model does not provide heating due to the green roofs at night; but instead, heating is provided by the heat stored in the impervious roof building materials. Despite this simplification, the model fluxes were still in reasonable agreement with measurements for Melbourne, Australia (Coutts et al., 2007).

TAPM can run for high-resolution (1 km grid cells) and downscale as 30, 10, 3, and 1 km nesting grid levels and each nesting grid consists of 25 × 25 horizontal grid points. Lateral boundary conditions for the 30 km simulation were provided by NCEP reanalyses (Kanamitsu et al., 2002). Vertically, grids extended up to 8 km above the ground. The relatively small 25 × 25 grid size was motivated by providing a simulation better constrained at the boundaries (i.e., its simulations reasonably match observations from weather stations), and its simulation efficiency is high. The efficiency saved significant computation time over the 10-year simulation period. Some simulations were undertaken with larger grid domains for a) 50 × 50 domain with 1 km × 1 km resolution and b) 25 × 25 with 3 km × 3 km resolution to test whether the predicted temperature changes between two scenarios are independent of the grid size used for the model. TAPM has limitations for choosing big outer grids (e.g., 150 km × 150 km domain at 1 km^2) as it violates model assumptions as discussed in TAPM user manual (Hurley, 2008a). Larger domains are often preferred for reducing the impact of lateral boundaries on the simulation results (Larsen et al., 2013). The 25 × 25 grid configuration was found to produce results more consistent with observations by having a reduced bias (see Appendix B for results). Simulations with the larger domain produced results qualitatively consistent with the predictions of the smaller domain but with increased bias. Hence, the 25 × 25 grid size results are reported in this paper. TAPM uses 38 land-use types based on U.S. Geological Survey data, and Australian terrain height data were obtained from Geoscience Australia. Synoptic-scale meteorological data were obtained from the Australian BoM (Hurley, 2008a). Although a drawback with our study is using a single modelling system, the TAPM results have also been compared with other modelling studies reported in the literature where appropriate.

2.3. Experimental design

While planning the experiments, we considered a sensitivity analysis in the same study area as Herath et al. (Herath et al., 2021). Based on these results, highly correlated urban surface parameters with urban heat were selected as variables, and experiments were designed to evaluate the impacts of urban green infrastructure (UGI) and reflective roofs on temperature indices. Since the CBD has a higher roof density, it is advantageous to use green and cool roofs for strategic adaptation planning. Green roofs are a promising adaptation strategy that provides a cooling effect to surrounding air temperature during day and nighttime, in summer, and during heatwaves across different climatic regions (Herath et al., 2018a; Imran et al., 2018; Herath et al., 2018b; Sharma et al., 2016). In addition, more green roofs associate with a higher reduction of UHI and roof surface temperature (Imran et al., 2018; Sharma et al., 2016). Cool roofs with high-albedo materials reflect more incoming solar radiation and absorb less heat than low-albedo materials during the day (Santamouris et al., 2011; Broadbent et al., 2021). Considering the evidence from Sharma et al. (Sharma et al., 2016) that green and cool roofs efficiently provide more cooling in highly urbanised regions with more roof area, we planned green and cool roofs for high-density Melbourne CBD. Moreover, cool roofs can be an effective solution with proven climate benefits when considering irrigation and other limitations in different case studies (Imran et al., 2018; Sharma et al., 2016). In most studies, highly reflective cool roofs have been modelled with albedo values from 0.65 to 0.9 (Imran et al., 2018; Santamouris et al., 2011; Gul et al., 2018). Evidently, as albedo values increase, cooling capacity increases (Herath et al., 2021), but having albedo higher than 0.85 is unrealistic. Limitations, such as the degradation of coating and roofing materials and the deposition of dirt on roofs, make the higher albedos impossible to implement (Bretz and Akbari, 1997). Considering timely degradation, discoloration, and dirt deposition, a 0.7 albedo is much more practical than extreme albedo values to maintain in an urban context.

Among other significant limitations imposed by costs, maintenance, and irrigation, another potential consideration for Melbourne is the competition of green and cool roofs against solar photovoltaic (PV) systems. Furthermore, a pre-planned and constructed city inevitably faces limitations when introducing new infrastructure by retrofitting the conventional built environment, as the planners have to consider and assess the feasibility of existing infrastructure to design for ecological use. For example, the transformation feasibility of an existing roof to a green roof should be weighed through building and roof characteristics, including the structure and the age of the building, slope and the bearable load of the roof (Joshi et al., 2020; Li and Yeung, 2014). Along with more limitations over implementation, justification for fractional quantities selection of variables is mentioned in detail in Section 4.5. Our prior study in Melbourne showed that green roofs are more effective than cool roofs in temperature mitigation at night and cool roofs provide higher cooling than green roofs during the day (Herath et al., 2021). Considering the trade-offs and the different diurnal effectiveness, we proposed limiting the green roof cover to a maximum of 50 % and allowing cool roofs to occupy the remainder.

The values for the control were adopted on the default values in the TAPM based on Coutts et al. (Coutts et al., 2007). The ratios of the different surface parameters were changed individually and combined to create scenarios (Table 1) to observe the impacts on the temperature variables. Every scenario was simulated with TAPM for 10 years, from 2011 to 2020. As discussed in the introduction and Section 4.5, some representation of irrigation is required; otherwise, the green roof dries out, and the vegetation is ineffective at cooling. Here irrigation is represented by a simple relaxation system that restores soil moisture to 75 % of the wilting and 25 % of the saturated soil moisture over a period of 24 h.

3. Model calibration

As depicted in Fig. 1, the grid centre was placed at the coordinates aforementioned CBD centre (37.8146°S, 144.9632°E). The modelling area was downscaled over 4 levels of 30, 10, 3, and 1 km nesting grids. All simulations used 1 month of spin-up time to minimise the impacts of the initial conditions. In the simulations, the ability of the TAPM to reproduce the meteorological and energy budget values was verified by model calibration. We have validated all the aspects of TAPM in normal conditions. The

Table 1
Experimental design for planning scenarios, including parameters for representing ground-level vegetation (T), green roofs (G), and changes to albedo to represent cool roofs (C).

Scenario name	Description of changing parameters		
	Urban trees - T (%)	Green roofs - G (%)	Cool roofs – C (Roof albedo)
S1 (control)	0	0	0.2
S2	0	0	0.45
S3	0	0	0.7
S4	0	25	0.2
S5	0	25	0.45
S6	0	25	0.7
S7	0	50	0.2
S8	0	50	0.45
S9	0	50	0.7
S10	5	0	0.2
S11	5	0	0.45
S12	5	0	0.7
S13	5	25	0.2
S14	5	25	0.45
S15	5	25	0.7
S16	5	50	0.2
S17	5	50	0.45
S18	5	50	0.7

green roof model has not been evaluated against observed data for Melbourne, although the parameters are based on values used by vegetation parameterisations from the literature. This is appropriate as process-based model predictions, which can be improved with real-world field tests in Melbourne. Therefore, the simulated (SIM) daily T_{max} and T_{min} values for 2 m above ground from the TAPM were compared with observational data (OBS) from five weather stations (WS) around the Melbourne metropolis for every 3 summer months from 2011 to 2020 (Fig. 1A, Table 2). For the observed data for T_{max} and T_{min}, each WS was directly obtained from the BoM databases measured daily for 24 h starting at 9 am. Simulated data were extracted from the corresponding or closest grid cross points in the TAPM. The corresponding data points from SIM were removed to OBS missing data in some WSs from the calculations.

The model proved to be valid for simulating Melbourne, with the smaller mean bias values for T_{max} and T_{min} of 0.19 and −0.16 °C, respectively. Therefore, the daily summer T_{max} from the model was 0.19 °C warmer than the observations, and the modelled daily T_{min} was 0.16 °C cooler. The highest bias for T_{max} was observed at Olympic Park WS, and Melbourne Airport reported the highest bias for T_{min}. Among statistic model evaluation metrics, we used mean absolute error – MAE (which measures the average magnitude of the errors in predictions without considering their direction) and coefficient of determination - R^2 (which shows the goodness of fit of the model). With MAE, the average absolute differences between the observed values and the predicted values are 2.22 for T_{max} and 1.66 for T_{min}. Both values generally represent low values which prove the ability of the model to fit the dataset. From R^2 for T_{max} of 80.07 % reveals that 80 % of the variability observed in the T_{max} variable is explained by the model, while 64.78 % of the variability is explained by the model for T_{min}.

4. Results and discussion

4.1. Overview

This section presents the analysis of results with extracted data from the finest grid level- 1 km and uses multiple temperature-related indices such as UHI, T_{ave}, T_{air}, T_{max} and T_{min} where necessary. First, all scenarios were compared with the control (S1) for UHI reduction and then for temperature variable changes. Next, each pair was compared to determine their different behaviours with temperature averages for the CBD. The average summer temperature (T_{ave}) was used as one of the temperature variables and was calculated from the daily simulated temperatures from 2011 to 2020. Finally, the 2 m air temperature (T_{air}), wind speed, latent heat, and sensible heat flux in the modelling area were compared with the control in three selected heatwave events for the scenarios with better performance.

4.2. Average seasonal Urban Heat Island effect in Melbourne

Since the UHI effect intensifies the negative thermal consequences during heatwaves, as mentioned above, this paper observed the difference between UHI temperatures for seasonal and during heatwaves. The most recent and accessible evidence for UHI Melbourne is based on 2018 vegetation cover and land surface temperature (LST) from Landsat 8 thermal infrared data (Sun et al., 2019). According to that study, the average UHI_LST in Melbourne ranges from −7.16 °C to 10.20 °C over different local government areas. Here we calculate the UHI for 2 m above ground air temperature using mesoscale modelling results as seasonal average UHI over 10 years.

In most scenarios, the existing UHI values exhibited statistically significant reductions. For example, S18 reduced the existing average UHI by 2.19 °C with a range of 0.94–3.92 °C. This reduction was mostly due to the drop in storage heat fluxes resulting in heat emissions at night. The statistical analysis that used ANOVA and the mean comparison that used Dunnett's method (S1 control) indicated significant differences ($p < 0.0001$) between the means of UHI (Table 3). Furthermore, these results coincide with the earlier findings of Imran et al. and Jacobs et al. for the Melbourne metropolitan area (Jacobs et al., 2018; Imran et al., 2018).

After validation, daily summer T_{min} values were extracted (as the most decisive impact of UHI is observed during the evening and nighttime (Martilli et al., 2020)) from the 1 km grid-level simulations. Temperature differences with T_{ave} were observed over 10 years for each scenario in the selected urban and rural areas. The UHI for Melbourne was calculated as the difference between the temperatures of the urban point (UP) and rural point (RP): UHI = T_{UP} - T_{RP}. For the analysis, to represent different urban characteristics, we extracted data from three locations: the CBD (CBD centre), UP1, and UP2 (inland and coastal points, respectively, in the urban generic [UG] area) from the same cross-section (Fig. 2). The daily T_{min} from the selected UP and two rural points (RP1 and RP2) were extracted from 2011 to 2020. Land-use characteristics of the CBD are represented by UP, while RP1 and RP2 describe different natural land-use types to interpret non-urban characteristics. The selection of RP1 was made purposely to locate in the same cross-section as UP and represents the 'shrubland: low mid-dense' land-use type. For RP2, inland 'grasslands with mid-

Table 2
Bias of maximum and minimum temperatures (T_{max}, T_{min}), calculated between the simulated and observed weather station values of the control scenarios from 2011 to 2020.

Weather station		Temperature bias (°C)		MAE		R^2%		Data availability %	
Name	ID	T_{max}	T_{min}	T_{max}	T_{min}	T_{max}	T_{min}	T_{max}	T_{min}
Olympic Park	86338	1.52	0.20	2.43	1.29	79.65	70.76	100	100
Melbourne Airport	86282	−0.59	−0.73	2.24	1.86	79.17	63.60	100	100
Viewbank	86068	−0.42	0.61	1.98	1.70	81.93	67.92	100	99.2
Essendon Airport	86038	0.71	−0.39	2.31	1.74	79.23	64.15	99.8	99.8
Moorabbin Airport	86077	−0.29	−0.50	2.13	1.69	80.36	57.47	100	98.8
Mean		0.19	−0.16	2.22	1.66	80.07	64.78	100	99.6

Table 3
Means, mean differences and standard deviations for temperature analysis for the CBD (from left: mean for average summer temperature, maximum temperature, minimum temperature, and air UHI). Except for S1, all mean values are listed as the d difference between S1 and scenario.

Level	Scenario	T_{ave}	T_{max}	T_{min}	*UHI*
S1		21.970 (1.48)	27.019 (2.00)	16.463 (1.15)	2.932 (0.63)
	S2	0.318 (1.45)	0.486 (1.96)	0.184 (1.14)	0.097 (0.59)
	S3	0.846 (1.41)*	1.143 (1.93)*	0.578 (1.14)*	0.287 (0.58)*
	S4	0.295 (1.45)	0.194 (1.98)	0.351 (1.14)	0.156 (0.59)
	S5	0.572 (1.43)	0.568 (1.97)	0.534 (1.14)*	0.253 (0.59)
	S6	1.037 (1.40)**	1.152 (1.93)*	0.875 (1.14)**	0.405 (0.59)*
	S7	0.604 (1.43)*	0.303 (1.99)	0.826 (1.14)**	0.409 (0.58)*
	S8	0.857 (1.42)*	0.645 (1.97)	0.998 (1.14)**	0.516 (0.57)**
	S9	1.179 (1.40)**	1.041 (1.94)*	1.246 (1.14)**	0.723 (0.59)**
	S10	0.059 (1.48)	0.073 (1.99)	0.051 (1.14)	0.051 (0.62)
	S11	0.464 (1.45)	0.638 (1.96)	0.294 (1.14)	0.147 (0.6)
	S12	1.016 (1.40)**	1.333 (1.91)*	0.694 (1.13)*	0.338 (0.58)*
	S13	0.375 (1.45)	0.266 (1.99)	0.418 (1.14)	0.203 (0.59)
	S14	0.701 (1.43)*	0.709 (1.96)	0.618 (1.14)	0.302 (0.58)*
	S15	1.127 (1.40)**	1.237 (1.93)*	0.932 (1.14)*	0.465 (0.58)**
	S16	0.722 (1.43)*	0.469 (1.99)	0.863 (1.13)**	0.483 (0.58)**
	S17	0.954 (1.41)**	0.773 (1.97)	1.015 (1.13)**	0.575 (0.58)**
	S18	1.244 (1.39)**	1.124 (1.95)*	1.248 (1.12)**	0.745 (0.56)**

* For significant p-values (<0.05) from Steel test to compare means of the scenarios with the control S1 (after significant p-value from one-way ANOVA tests for each).
** For p-values <0.0001: (UHI was represented as urban – rural).

dense tussock' land type was selected. Therefore, the UHI (calculated from 2 m above-ground air temperature) for the Melbourne CBD, was estimated as 2.93 °C (averaged from UP to RP1 and UP to RP2) with a range of 1.63–5.3 °C. Thus, Melbourne is 2.93 °C warmer than the surrounding suburbs on summer nights, proving the UHI effect.

4.3. Heat mitigation during extreme climate conditions

4.3.1. Mitigating excessive heat of Urban Heat Island effect during the heatwaves

Fig. 3 depicts the simulated diurnal variation of existing seasonal UHI (UHI_S) behaviour in Melbourne and how it sharply increased during the heatwave event in 2009 from UHI_{hw}. Higher UHI values were observed during summer at night. The UHI during the heatwave has increased around 3 °C over the average seasonal UHI. The highest temperature difference between urban and rural was reported during 3–4 am. The three scenarios, S9, S12 and S18, made considerable reductions in diurnal UHI graphs during the day and night.

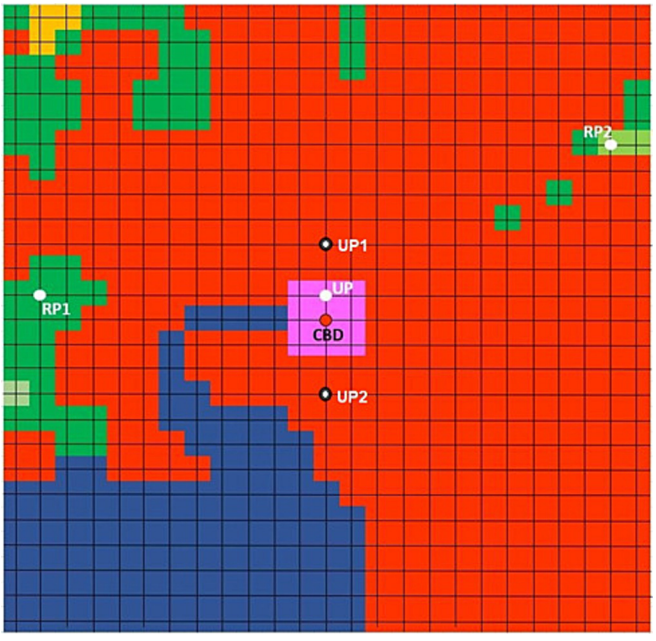

Fig. 2. TAPM 1 km grid window for Melbourne metropolitan (Data extraction points for UHI calculations: RP1 and RP2 – 'Rural points' and UP – 'Urban point'; Data extraction points for analysis: CBD – Centre of the CBD and UP1 and UP2 – Inland and coastal urban points, respectively.

4.3.2. Number of hot days and nights

Based on the method described by Chapman et al. (Chapman et al., 2018), we determined the extreme threshold temperatures for each summer. Hot days in the CBD were specified when the T_{max} in the CBD was equal to or higher than the 97.5th percentile of the T_{max} of rural points (average of two rural points) in the S1-control. Hot nights were determined by using the same method as that for T_{min}, as shown in Table 4 (Appendix A). S1 recorded two average hot days and 5.6 hot nights per summer under the control scenario. We compared the means of all scenarios by using Dunnett's test (S1-control, significant level $p < 0.05$), and the average number of hot days was significantly reduced in the scenarios- S2, S3, S5, S6, S8, S9, S11, S12, S15, S17, and S18 (basically all items with a cool roof albedo > 0.2) compared with S1, and S4 increased the mean to 2.1 (not statistically significant). Only scenarios S9 and S18 significantly reduced the average number of hot nights than S1 (5.6 nights per summer), where both scenarios represented cool roofs with an albedo of 0.7 and green roofs with 50 % cover. S12 reported a minimum average of 0.3 for hot days; for S18, 2.8 average hot nights was the minimum record.

As shown in Table 5 (Appendix A) for the reduction of hot days and nights, all scenarios with the maximum realistic albedo of 0.7 had a significant reduction in hot days. High albedos prevent energy absorption by promoting the reflection of incoming solar radiation. This phenomenon leads to lower surrounding temperatures (Li and Norford, 2016; Taha, 1997). S9 and S18 have mutually claimed 50 % of green roofs and albedo 0.7 cool roofs and, a significant reduction in the number of hot nights was observed. These results support findings in the literature that urban vegetation promotes cooling during nighttime and reduces the UHI impacts on Melbourne (Herath et al., 2021; Jacobs et al., 2018).

4.3.3. Behaviours of temperature variables and energy budget components during heatwave events

Melbourne experienced three distinct heatwaves in our study period (2011 – 2020): in 2014 (14–16 January), 2018 (considered summer 2019, 6–8 December), and 2019 (28–30 January). An unprecedented heatwave occurred in 2009- the south-eastern Australian heatwave started on 25 January and lasted for 16 days. Our results showed that the average air temperature during the 2009 heatwave was ~12 °C higher than the seasonal summer average temperature. The 10-year average maximum (27.02 °C) and minimum (13.79 °C) temperatures were exceeded during the heatwave by 15 °C (T_{max}), and 11.4 °C (T_{min}). The magnitude of these extreme heat events highlights the need for urgent mitigation strategies to protect vulnerable urban populations. Although the two incidents in 2019 exceeded the thresholds, the temperature values were not comparatively significant in 2009. Although the 2009 heatwave was out of the selected timeframe, it best represented the worst-case scenario with the highest recorded temperatures. Therefore, we simulated the behaviour of air temperature with different wind speeds and energy budget components (e.g., latent and sensible heat), during the 2009 heatwave in Melbourne. We used hourly data for three heatwave days (72 h), and Fig. 4 illustrates the average spatial changes during the heatwave (scenario minus control). For the existing conditions (S1) in Melbourne, T_{ave}, T_{max}, and T_{min} were 34.31, 43.00, and 27.90 °C, respectively, for the 2009 heatwave.

Scenario selection in Fig. 4 was justified as S3 consists of 0.7 cool roofs only; S7 with 50 % F2, green roof only; S10 with 5 % F1, urban trees only; S12 shows the best performance for T_{max} with F1-Urban trees and F3-cool roofs, and finally, S18 performs the best for T_{min} consists of all strategies- F1, F2, F3. Each scenario was compared with control S1 by using a paired *t*-test to observe a significant change (depicted as dark-coloured dots in Fig. 4). Negative values represent the reduction in each variable value

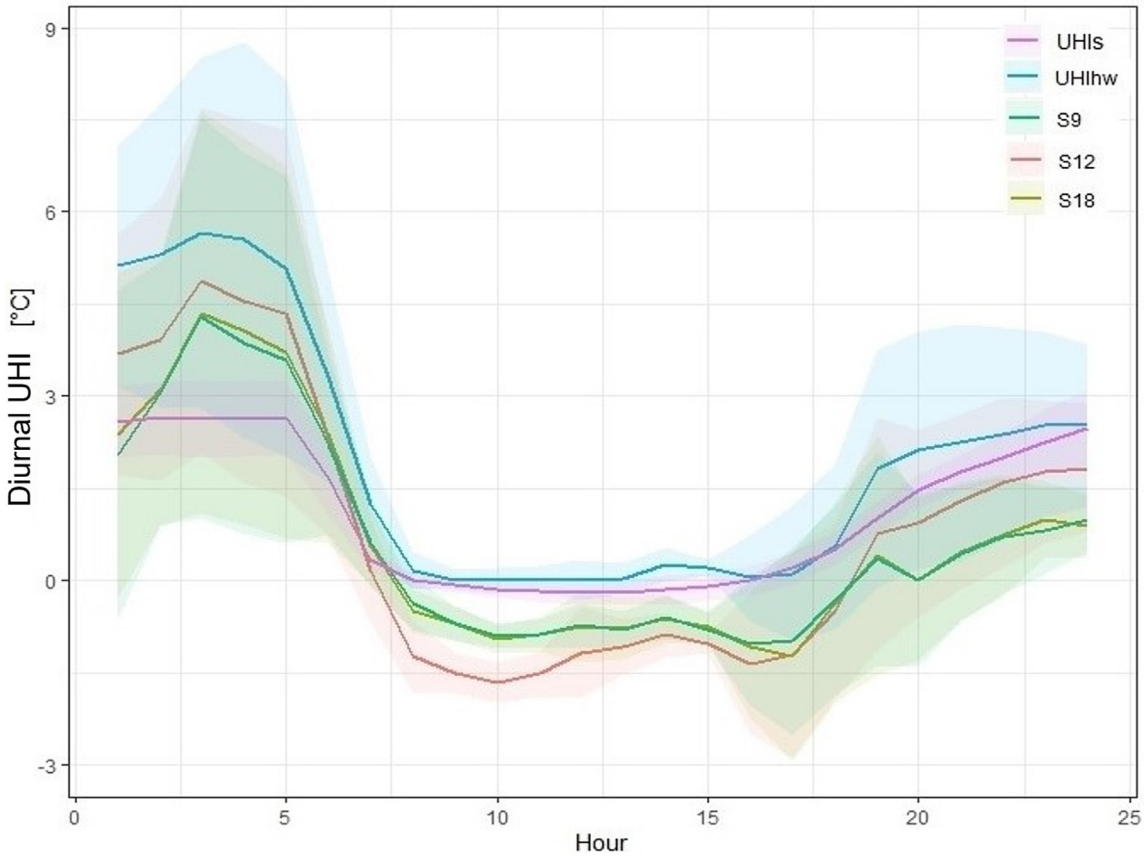

Fig. 3. The diurnal UHI (measured from air temperature at level of 2 m above-ground) variation by different scenarios. UHIs - Seasonal UHI (calculated average from 2011 to 2020), UHIhw – UHI during 2009 heatwave (average values for 3 heatwave days, represent the control), S9 (T = 0, G = 50 %, C = 0.7); S12 (T = 5 %, G = 0, C = 0.7) and S18 (T = 5 %, G = 50 %, C = 0.7). The shaded area represents 1 SD (standard deviation).

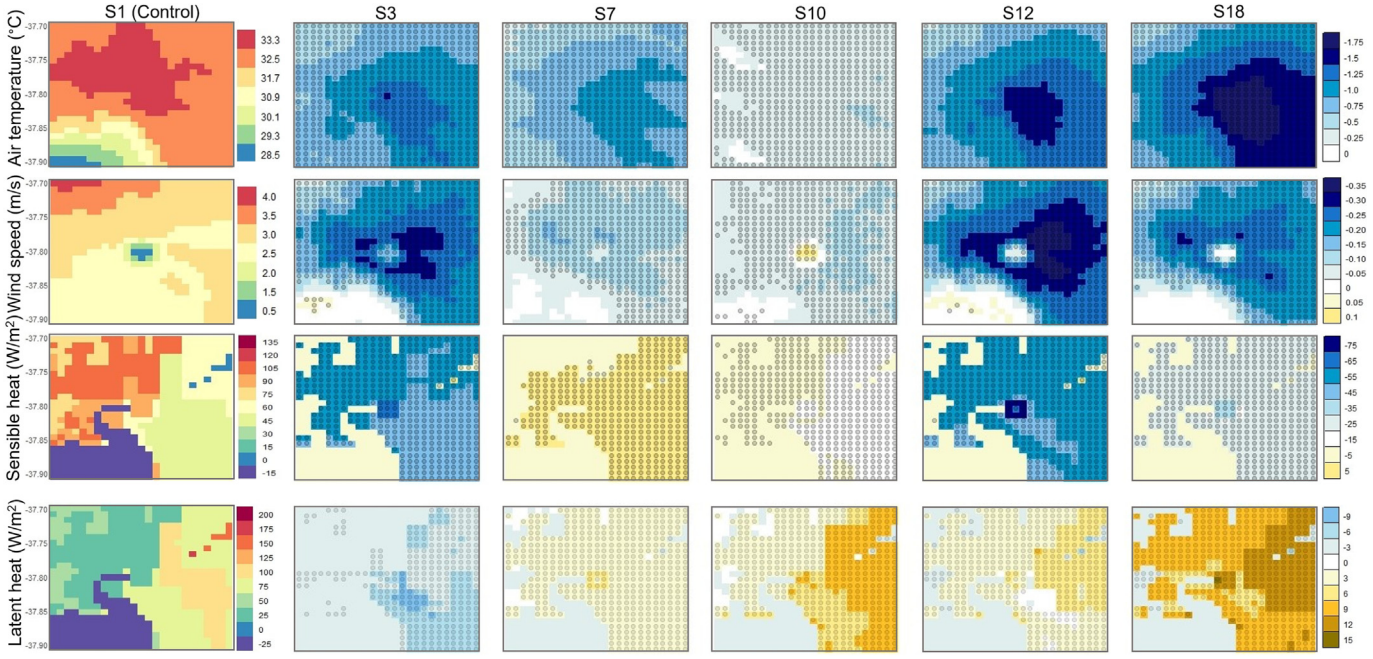

Fig. 4. Spatial maps for Melbourne for 2009 heatwave with values of the variables for S1 (control) and the differences of selected scenarios from S1. The difference is calculated as scenario minus the control. (Dark dots indicate the significant change between the control and scenario: CL- 95 %), Scenarios: S1(control, T = 0, G = 0, C = 0.2); S3 (T = 0, G = 0, C = 0.7); S7 (T = 0, G = 50 %, C = 0.2); S10 (T = 5 %, G = 0, C = 0.2); S12 (T = 5 %, G = 0, C = 0.7) and S18 (T = 5 %, G = 50 %, C = 0.7).

compared with S1. The measured temperature variables in different urban LCZs evidently showed differences. T_{air} was reduced to a maximum of 2 °C, and S18 offered a reduction metropolitan-wide, especially around the CBD. Notably, areas with higher temperatures showed lower wind speeds, higher sensible heat, and lower latent heat fluxes than low temperature areas. S10 showed slight or null declines for T_{air}, wind speed, and sensible heat; however, with increased urban trees, S10 offered a range map for latent heat with evaporation. Cool roofs seemed responsible for reducing sensible heat rather than the other scenarios, with evidence in S3 and S12. Roofs with higher albedos (S3) had significantly reduced latent heat fluxes. This reduction directly affects the energy budget by reducing the sensible heat flux and consequently decreasing net radiation and the surface temperature (Herath et al., 2021). S3 was arranged with 100 % cool roofs that did not achieve the highest reduction but achieved the maximum reduction when combined with urban trees in S12. Particularly notable is that S12 appeared to be an extreme case where a cool roof with a high albedo and no green roof was sufficient to minimise the sensible heat flux, partly due to the reduction in wind speed, and partly by reducing surface temperature. As shown in the results, S12 recorded the highest reduction in average seasonal T_{max}, which was measured during the day.

Meanwhile, Fig. 5 depicts the diurnal variations of the energy budget components during the heatwave extracted from the Melbourne CBD centre, which is compared with the seasonal summer averages. During the heatwave, the energy budget components in the CBD location showed higher latent heat, net radiation, and storage heat fluxes with lower sensible heat than the seasonal averages. S18 increased the latent heat flux, with a higher vegetative ratio of 50 % for green roofs with 20 % (5 % increase) urban trees. Conversely, S12 maintained the lowest sensible heat and net radiation values during the day. The significant lower sensible heat values in the diurnal cycle in Fig. 5A are discernible for S12, unlike S18 had 50 % green roofs as the only difference from S12. Higher albedos have a bigger impact on lowering temperature compared to increasing evapotranspiration. The presence of green roofs increases evapotranspiration while at the same time noticeably reducing the albedo. Removing green roofs in the model causes two consequences: evapotranspiration becomes unavailable for the surface energy budget and the lower albedo of the green roof is replaced with the much higher albedo of the cool roof. In UCLEM, heat storage is provided by the impervious roof component, whereas no heat is stored by the green roof. Therefore, in S12, the change in albedo reduced the heat being absorbed by the roof to a much greater extent than the reduction in evapotranspiration. This led to an overall cooling in the roof surface temperature with a cool roof. The net result is that the model predicts a reduction in sensible heat flux with respect to a cool roof, as the change in albedo had a larger impact on the energy budget than the changes in latent heat flux. Notably, the sensible heat during the heatwave (S1) was lower than the seasonal average. However, excessive heat from the net radiation appeared to have remained in the system as stored heat. Thus, all three scenarios can reduce or increase air temperature (Li and Norford, 2016). Therefore, for S12 and S18 scenarios, TAPM predicts lowered fluxes with upward curves to almost seasonal averages, directly showing thermal comfort benefits for city occupants.

4.4. Heat mitigation under average climate conditions

4.4.1. Seasonal temperature changes with scenarios

Summer T_{ave} changes for each scenario were observed using the data extracted from the centre of the CBD. For S1, the existing urban condition which is the mean for T_{ave} for 10 years was 21.97 °C and ranged from 18.40 to 25.66 °C. The average 10-year T_{max} was 27.02 (22.36–31.99) °C, and T_{min} was calculated as 16.46 (13.79–18.64) °C. The p values of all three ANOVA tests for T_{ave}, T_{max}, and T_{min} were reported as significant (<0.0001), indicating differences in the mean temperature values among scenarios. The existing setup for Melbourne (S1) was then compared with the other scenarios by using Dunnett's test (Table 3). Each scenario exhibited a different behaviour for different temperature variables. However, the p-values of S3, S6, S9, S12, S15, and S18 were significant compared with S1 for all temperature measurements, T_{ave}, T_{max}, and T_{min}. We selected the aforementioned six scenarios for further analysis among all significant scenarios.

4.4.2. Seasonal variations of temperature and energy budget components among LCZs (urban types)

This study used three receptor points in two urban types: the CBD with high-rise and compacted buildings (LCZ1) and UP1 and UP2 in general urban areas (Fig. 2) with low-rise buildings (LCZ3) characteristics. All three points were chosen on a straight line to avoid biases, where UP1 is

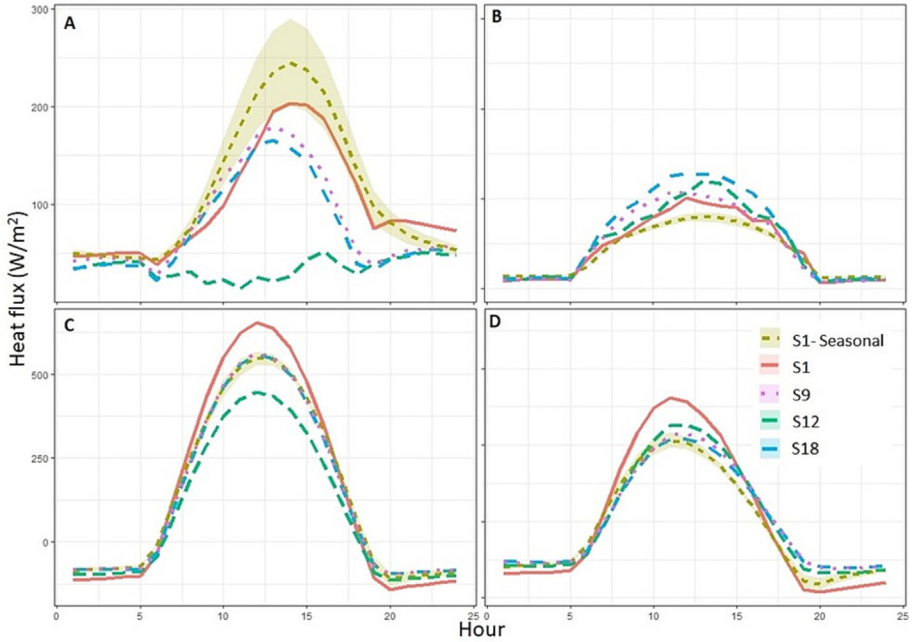

Fig. 5. Diurnal variation of energy budget components in the CBD location during 2009 heatwave; A: sensible heat flux; B: Latent heat flux; C: Net radiation, and D: Storage heat flux for selected scenarios (S1- (control, T = 0, G = 0, C = 0.2; S9-(T = 0, G = 50 %, C = 0.7); S12- (T = 5 %, G = 0, C = 0.7) and S18- (T = 5 %, G = 50 %, C = 0.7) compared with Seasonal S1).

the inland location and UP2 represents near-coast urban locations. Martilli et al. pointed out that analysing temperature differences within different urban areas (various LCZs) is more meaningful for temperature evaluation studies than focusing on urban-rural differences. Below we discuss the temperature and energy budget variations within different urban types in Melbourne.

Urban surfaces release terrestrial radiation slowly, and vegetative surfaces promote less trapping of solar radiation than urban surfaces and rapid release of terrestrial radiation (Papangelis et al., 2012). Studies have established that rural areas consume 50 %–60 % of available energy as latent heat while budgeting 15 %–30 % as sensible and subsurface heat fluxes at noon (Mcpherson, 1994). However, in cities with fewer vegetative surfaces (5 %–20 %) and higher ratios of impervious surfaces, 30 % of available net radiation is absorbed as latent heat. Therefore, more energy remains as sensible heat (45 %) to heat the air at noon (considering it as an irrigated hypothetical city) (Mcpherson, 1994). After implementing the mitigation strategies, S12, with the total roof surface of cool roofs and 20 % urban trees showed the lowest sensible heat and net radiation curves. Cool roofs have been proven to reduce the net radiation and sensible heat more effectively than green and conventional roofs (Imran et al., 2018). Moreover, S18 drew the highest curve for latent heat with greener surfaces because green roofs are known to convert net radiation into latent heat with evapotranspiration (Fig. 6) (Imran et al., 2018; Mcpherson, 1994). This scenario decreased the net radiation by approximately 125 Wm^{-2} in all urban locations of the CBD and UPs. Urban trees increased by 5 %, promoted evapotranspiration, provided shading, and decreased the incoming solar radiation. In UCLEM, shading reduces the amount of shortwave solar radiation absorbed by the canyon walls, effectively modifying the canyon geometry proportional to the height of the vegetation. Hence to first-order the surface temperature is reduced by the reduction in solar radiation heating the walls of the canyon. Additionally, 50 % of roofs as green roofs promoted latent heat and reduced sensible heat simultaneously, and the remaining roofs reflected the incoming solar radiation. Therefore, S18 is an excellent combination for reducing the net radiation of the system. However, implementing scenarios always yields better balanced curves for the energy budget components than the existing S1.

With high heat-absorbing urban materials, CBD promotes heat storage which is released during the night and eventually increases T_{min}—the nighttime temperature (Environmental Protection Agency, 2011; Wonorahardjo et al., 2020). The results of the seasonal summer averages for the existing temperature indices demonstrated that T_{min} showed a statistically significant difference in the CBD from both UPs (similar for UPs) and that T_{max} and T_{ave} were nonsignificant. The high T_{min} in the CBD can be explained by Fig. 6, because the storage heat fluxes were higher in the CBD than in the UPs. The energy stored from solar radiation is released from the construction materials of buildings and all impervious surfaces during the night by increasing T_{min} (Imran et al., 2019b). This difference, even between high- and low-density urban areas, created temperature gradients, leading to UHI, and we can predict that this will intensify in rural settings. Adding the S12 and S18 scenarios to the study site did not cause significant mean changes in T_{max} and T_{ave}; however, the temperature drops were still observable. S12 also showed significant differences in T_{min} among all three urban locations: CBD, UP1, and UP2. Notably, S18 reduced the mean values of T_{min} without creating temperature gradients in the urban profile. In the UPs, higher T_{max} was recorded, and this occurred at higher wind speeds than in the CBD. Urban generic areas were recreated in the model with low-rise buildings of similar height and low surface roughness to represent less drag on the wind, allowing for increased wind speeds (Wever, 2012). High wind speeds caused low turbulent mixing and prevented the heat from being carried away. This will increase the T_{max} of the study area and intensify the UHI effect (Gunawardena et al., 2017).

Fig. 6 presents the hourly variations in the energy budget components (net radiation, storage, latent heat, and sensible heat flux) for 24 h. The seasonal mean values were used from 2011 to 2020 for the selected scenarios

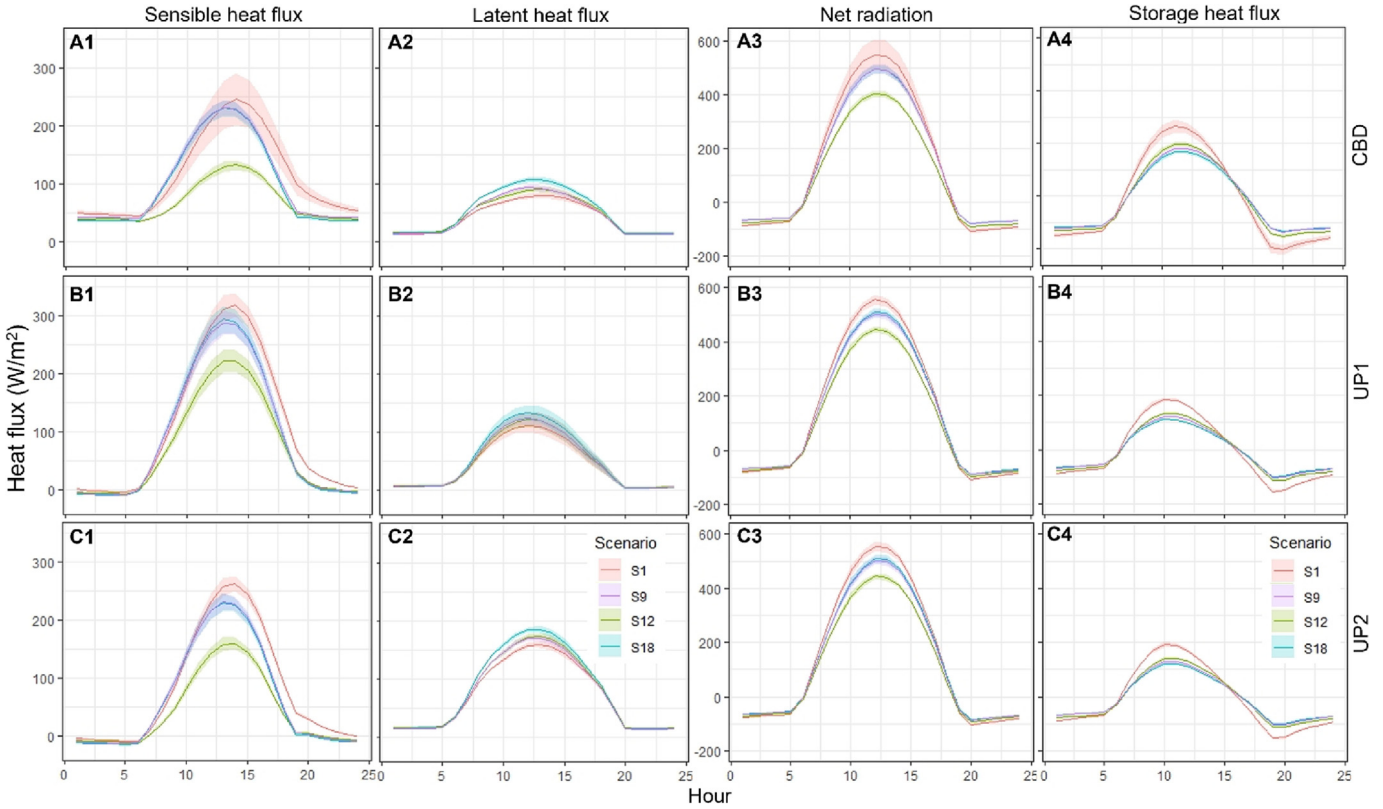

Fig. 6. Seasonal mean for diurnal variation of sensible heat flux (left:1), Latent heat flux (left:2), Net radiation (right:3) and storage heat flux (right:4) for summer 2011–2020 for selected scenarios (S1-(control, T = 0, G = 0, C = 0.2); S9 (T = 0, G = 50 %, C = 0.7); S12 (T = 5 %, G = 0, C = 0.7) and S18 (T = 5 %, G = 50 %, C = 0.7)) at A: CBD, B: UP1 and C: UP2.

for three urban locations: CBD, UP1, and UP2. The scenarios – S12, and S18 were chosen because they showed the highest reductions for temperature indices of T_{max}, T_{min}, T_{ave} and UHI, while S9 acts almost similar to S18. The sensible and latent heat fluxes increased during the daytime and decreased at night. As shown in B1, UP1 reported higher sensible heat fluxes during the day than CBD and UP2. This difference could be due to its spatial variability: UP1 is located farthest from the sea and is surrounded by urban surface characteristics. The minimum sensible heat flux was reported with S12 for all urban locations because 100 W/m^2 was constantly reduced by S12. S12 corresponded to a purely cool roof with a high albedo of 0.7 (and a 5 % increase in urban trees), whereas the other scenarios- S9 and S18 had 50 % green roof coverage that effectively reduced the roof area with 0.7 albedo, but potentially included more evapotranspiration. Despite the minimum impact of 5 % urban trees, the cool roofs with a high albedo could cause the low sensible heat for S12. S9 and S18 overlap for each graph (Fig. 6); therefore, regardless of the 5 % increment in urban trees in S18, both scenarios acted similarly, involving the energy budget. Every scenario showed higher latent heat than S1, promoting cooling in the urban area. The maximum latent heat was reported in S18 through increased evapotranspiration, with the maximum vegetation fraction among all scenarios.

Urban points were graphed with higher sensible and latent heat fluxes than the CBD in the existing energy balance for seasonal summer averages in the modelling area. However, the CBD had higher storage heat fluxes than the UP locations, which might be due to the dense and high-rise building characteristics. The characteristics of the CBD differ from those of UG areas: the CBD has more built-up and road ratios than it has vegetative surfaces, and UG areas are less built-up with more vegetation than the CBD. Storage heat is a crucial cause of the UHI effect, and this storage occurs because of the thermal conductivity and heat capacity of urban surface materials and the greater 3-D surface area in a city (Oke, 1988). According to Fig. 7, the CBD has higher storage energy than UP1 and UP2, and this difference leads to UHI at night. However, a reduction was observed with S9, S12, and S18, whereas S18 always showed the lowest curve. This observation can be explained by scenario S18 having the greatest urban vegetation ratio (no energy is stored in the vegetation canopy in the UCLEM) and the highest cool roof albedo. The net radiation peaked at approximately noon, and the peak was almost the same for all three urban locations. However, the curve was lowered the most in S12 by reducing the total net radiation to approximately 125 W/m^2 for the CBD, UP1, and UP2.

4.5. Operationalisability of these scenarios in urban areas

4.5.1. Practical and cost limitation

We acknowledge that effectiveness is used in different ways in literature. For example, the effectiveness of urban blue-green infrastructure (UBGI) strategies for mitigation purposes is defined differently as in Imran et al. (2018), Imran et al. (2019a), Sharma et al. (2016), Jiao et al. (2017), Lin et al. (2013), Li et al. (2014), Di Giuseppe and D'Orazio (2014), Pugh et al. (2012), and Chen et al. (2016). Krayenhoff et al. used two indices to measure effectiveness, vegetation cooling effectiveness (VCE) and albedo cooling effectiveness (ACE), to quantify the cooling ability of strategies that use vegetation and higher albedo values (Krayenhoff et al., 2021). Bai raised the necessity of measuring the functional effectiveness of UBGI against conventional engineering-based infrastructure (Bai, 2018). We argue that effectiveness needs to be defined combining functional performance and operationalisability, including cost-effectiveness and feasibility. In this study, the term effectiveness is used to refer to the degree of cooling effects delivered combined with operationalisability or feasibility, in relative terms, of the combined strategies. However, a detailed cost evaluation is beyond the scope of this paper and is planned for future work.

In the literature, most of the modelling studies have tested the extreme fractions to observe the impact of changing variables, such as zero and 100 % (Chapman et al., 2018; Herath et al., 2018b). Despite the promising results for success, most scenarios cannot be practically implemented on the ground, and as such, questions remain regarding their operationalisability. For example, there are constraints in financeability and design standards for installation, maintenance, space, and resources (e.g., water). Moreover, some concerns regarding ownership of the property, and socio-economic

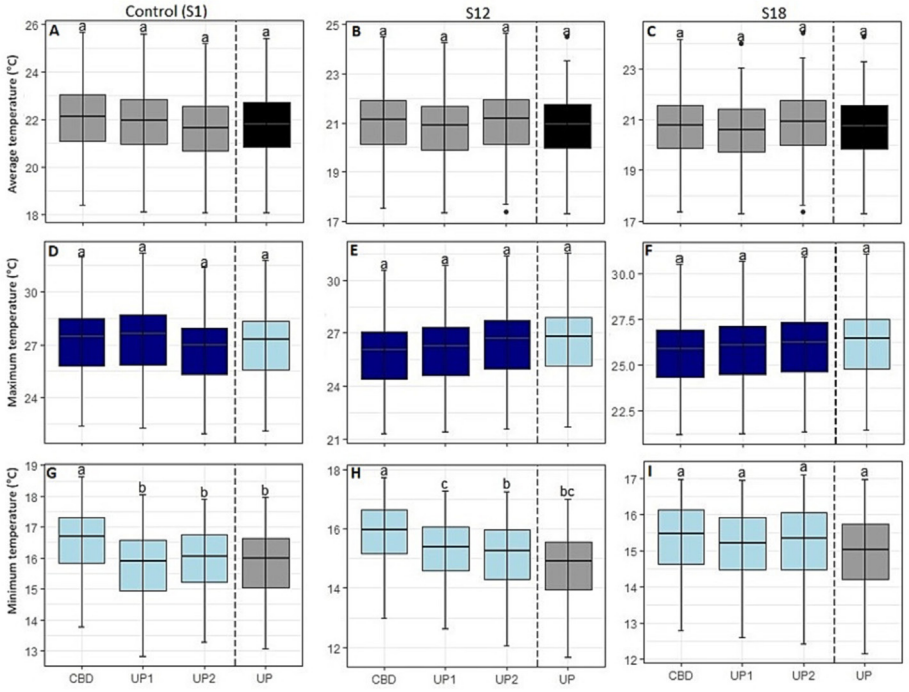

Fig. 7. TAPM mean summer temperatures (2011–2020) for average, maximum and minimum temperature (whiskers for error bars) for different urban types in Melbourne; A, D and G represent the existing condition for Melbourne (control); B, E, H for S12 (T = 5 %, G = 0, C = 0.7) and C, F, I for S18 (T = 5 %, G = 50 %, C = 0.7); (UP represents the average value for UP1 and UP2). The letter "a" indicates when the change of temperature variables was not significant at $p < 0.05$, and "b" and "c" indicate significant differences of means among different urban locations (performed in a Tukey multiple means comparison).

considerations, such as public perception, policy constraints, administrative restrictions, technology, and innovation are also significant constraints on implementation (Zuniga-Teran et al., 2020; Reimer and Rusche, 2019; Onori et al., 2018). Because operationalisability is one of the objectives of this study, we concentrated on selecting feasible and optimum implementation ratios through a literature survey for Melbourne.

Melbourne is planning a low-carbon city with greener spaces to cope with the effects of climate change (Victoria State Government, 2017). *Plan Melbourne, 2017–2050*, is policy documentation that promotes increasing vegetation cover to 40 % (from 22 %) by 2040 (City of Melbourne, 2012) in city planning. Subsequently, a study of Melbourne demonstrated that >40 % vegetation was necessary to increase temperature reductions (Imran et al., 2018). Therefore, our experiments planned an affordable and most ambitious vegetation fraction of 43 % in the non-CBD (UG) area and 20 % in the CBD—a 5 % increase in the existing percentages of both areas to overcome the above limitations for irrigation and space availability. Moreover, irrigating urban green is a critical limitation as Australia's water availability is under pressure because of its low rainfall and rising population (ABS, 2008; Dey et al., 2019). In our model simulation, TAPM assumed the greening options to be well-irrigated with 100 % irrigation. Heusinger et al. quantified as an unrestricted irrigation condition on green roofs can reduce 48 % - 75 % of excess urban heat compared to black roofs, while sustainable irrigation conditions drop up to 15 % - 51 % in different cities (Heusinger et al., 2018). During heatwaves, soil moisture of substrate tends to drop critically, making cooling unsuccessful. Unirrigated green roofs dropped the heat reduction by 3 %, which causes more heating (Heusinger et al., 2018). Therefore, green roof plans should seek adaptive and innovative strategies to compete with water requirement stress during heatwaves and average conditions. For example, green roofs can use recycled greywater as a successful alternative to potable water (Fowdar et al., 2017; Prodanovic et al., 2017). Using different substrates with high water holding capacity (Grard et al., 2018), and modifying substrates with water retention gels (Young et al., 2017) are successful and manageable strategies to reduce irrigation water requirements to reach the saturated condition.

However, roof surfaces have multiple trade-off relationships because roof areas should facilitate solar PV, green roofs, and cool roofs. Recently, most households have been shifting to renewable energy, and Australia has planned for 2.2 million small-scale solar panels (Australian Energy Council, 2020). Therefore, green roofs must compete for space with solar panels. An alliance of solar panels with green roofs can produce up to 16 % more energy than plants from green roofs, provide a cooling effect with evapotranspiration and maintain solar panels at their ambient performance temperature (Barcelona City Council, 2015). Moreover, green roofs prevent the latching of suspended particles on solar cells (Barcelona City Council, 2015) by providing dry deposition of particulate matter from traffic pollution (Tong et al., 2016; Viecco et al., 2018). Our study did not include an alliance of green roofs and solar PV panels in the same space; however, we considered 50:50 availability for the same roof. Therefore, considering these trade-offs, this study maintains the green roof levels practically and adequately to provide maximum climate benefits.

The construction techniques, implementation, and maintenance of UGI require extra expertise, attention, and capital. For example, green roofs require higher life cycle costs than average for three main phases: installation, lifetime, and replacement. Green roofs have lower short-term investment returns than conventional roofs but excellent long-term returns (Downton, 2013; Chen et al., 2019). These high-cost requirements become limitations when there are widespread doubts regarding who would pay and how the initial and maintenance costs, retrofitting of existing buildings, irrigation, and plant nutrition would be conducted (City of Melbourne, 2017). Some municipalities (55 %) identified a lack of public funding as a major barrier to sustainable urban growth (Lindfield and Teipelke, 2017). To avoid these high-cost limitations linked to size, design, and type (Broadbent et al., 2021), strategies, such as small projects at the domestic level or do-it-yourself (DIY) installations, are being promoted among communities. The cost of a small green roof in Melbourne with reasonable access would cost 150–400 AUD/m^2 (according to the 2013 prices), excluding fees for designing, planning, permits from local councils, permits for lifts and cranes, demolition or relocation of existing infrastructure, and additional specific infrastructure, such as shade, decking, paving, and trailing (DEPI, 2014; Gibson, 2021). As empirical evidence, a 50 m^2 green roof installed in Coburg is valued at approximately AUD 30,000 which most architects consider a high budget (O'Donoghue, 2016). According to Wilkinson et al., each life cycle phase costs from AUD 19.08 to 215.76 for installation; AUD 0.49 to 2.83 for maintenance per m^2 and AUD 55.54 to 2.28, AUD 1.06 to 1.27 for demolition and replacement per square meter for building owners (Wilkinson et al., 2017).

Cool roofs are more advantageous than green roofs because the former has lower installation and maintenance costs and no irrigation needs (Imran et al., 2018; Sharma et al., 2016). Typical, conventional roofs have an albedo ranging from 0.1 to 0.3 (reflecting 10 %–30 % of incoming solar radiation, with the rest absorbing) (Wang et al., 2016), and cool roofs have high reflectivity with higher albedos than conventional roofs. Due to the high reflectivity of roofs, incoming solar energy tends to radiate back with cool roofs instead of being absorbed and transferred inside the building. This eventually reduces air conditioning costs while promoting thermal comfort and human health (Uni.Melbourne, 2011). Moreover, in addition to the cooling benefits, the maintenance of cool roofs is more manageable, and implementation costs are lower due to less sophisticated designs, reroofing, and retrofitting than green roofs (Uni.Melbourne, 2011; City of Melbourne, 2014). However, as proved in this study and some of the literature for Melbourne, cool roofs are only effective for daytime temperature reductions (Herath et al., 2021; Imran et al., 2018; Jacobs et al., 2018), and are highly beneficial during summertime (Macintyre et al., 2021). The Melbourne City Council promoted a building retrofitting project in 2010. The '1200 Buildings Program' aimed to improve energy (and water) efficiency by retrofitting 540 commercial buildings with higher roof albedos in Melbourne (City of Melbourne, 2014,2016). Therefore, cool roofs are effective, practical, and affordable for most temperate cities such as Melbourne.

4.5.2. Importance of using the reasonable maximum ratio

The results showed different heat reduction effectiveness for different scenarios. As demonstrated in this study, all parameters had the highest efficiency with the maximum cooling potential when greater ratios/values were applied. Increasing urban trees (F1) and green roof (F2) ratios have proven effective in urban environments because urban vegetative surfaces increase the moisture availability of the surrounding. Urban trees induce cooling via transpiration and shading (Meili et al., 2021; Taha, 1997; Krayenhoff et al., 2020). Every bit of urban vegetation contributes to heat reduction (Herath et al., 2021), and higher tree cover promotes a more significant cooling potential. For example, according to Imran et al. (2018), >40 % of total vegetation significantly reduces temperature. However, new studies show that the increment of urban trees after a certain level is associated with some limitations (Park et al., 2019; Meili et al., 2021). Since trees in the urban environment tend to alter the wind flow and urban aerodynamic roughness, they restrict heat dissipation (Meili et al., 2021). With well-irrigated urban trees, cooling happens with transpiration; however, restricted irrigation limits further cooling. Apart from these facts, we also focused on practical restraints in Melbourne, such as the existing fractions of buildings, roads, and other impervious surfaces. In Melbourne, built-up areas and ground-level vegetation cover occupy 65 % and 15 % of total CBD areas, respectively, and they are 45 % and 38 % in the UG area (Coutts et al., 2007), and what remains is 20 % and 17 % for roads in the CBD and UG, respectively. Assuming the ratios of roads remain constant, we considered the urban tree cover of 20 % and 42 % as reasonable maximums in the CBD and UG areas, respectively. These increased tree cover ratios led to a reduction in the T_{max} and T_{min} by 0.07 and 0.05 °C, but the reduction values were relatively small. In addition, the scenarios with a vegetation increase showed more substantial impacts on nighttime

temperature than on daytime temperature, which is consistent with findings in the literature (Herath et al., 2021; Imran et al., 2019a; Grimmond, 2007). When we changed only the vegetation ratio, the heat reduction of those scenarios was relatively small. However, heat reduction was significant during the nighttime with a maximum green ratio (e.g., 50 % green roofs). Our results proved that attention should be paid to diurnal cooling capacity as some scenarios' effectiveness varies day and night. However, this study did not aim to assess the seasonal cooling capacity, which could have different levels of effectiveness during summer and winter as confirmed by Krayenhoff and Voogt (2010).

In addition to the effectiveness, each parameter has different advantages and constraints. Operationalising plans with surface characteristics is always costly. Moreover, there are limitations to space availability for increasing tree canopy cover in canyons, urban parks, and gardens in existing cities. To overcome these limitations, planning should be case-specific. The feasibility of the selected plan should be evaluated by studying similar and different empirical evidence from different geographic locations. Choosing the most suitable parameters for a particular urban area should be financially sensible. For example, in cities where the cost of UGI, such as green roofs, is unaffordable, cool roofs and urban trees to mitigate daytime temperatures are still practicable. Planning UGI to reuse and recycle water and other resources is another means to be cost-effective, which could be efficient in a water-scarce context such as Australia. As we firmly grounded in this study, combined scenarios with high-albedo materials and vegetative surfaces are highly effective, and the best performance is achieved by overcoming most of the aforementioned limitations. Combined scenarios strategically alter urban plans to occupy reasonable maximum surface ratios while achieving maximum cooling benefits, which equally improves day and nighttime thermal benefits. These equal benefits eventually lead to excessive heat and UHI mitigation and directly to energy saving (Akbari and Konopacki, 2005).

For most temperature indices, such as T_{ave}, T_{min}, and UHI, the highest reductions were rendered by the combined scenario of 20 % vegetation, 50 % green roof, and 50 % cool roof with 0.7 albedo (S18), with a reduction of seasonal average T_{air} of 1.25 °C, and in the CBD, a maximum reduction of 2.1 °C during heatwaves. This scenario also showed preferable performances for T_{min} and UHI, making it the best strategy for mitigating UHI effects in Melbourne. Combined scenarios are most effective in terms of the maximum cooling benefit and can be cost-effective for Melbourne. This cost-effectiveness is enhanced when the costs are compared with the benefits of UGI because the added greenery from UGI can provide co-benefits, including many ecosystem services, and enhance the ecological value of the urban area. As discussed, when green roofs tend to be expensive and often impractical in an existing urban context, combining them with less expensive cool roofs can be a much more cost-effective strategy.

Recent urban literature suggests that urban planning should focus more on the spatial layout of the mitigation solutions with the allocation ratio. Most available case studies have reported plenty of successful case studies on microscale, but with the level of individual or isolated implications. However, urban planning requires confirmation over large-scale ecosystem integration in cities (Bai, 2018) before going for mitigation solutions at individual levels. Therefore, identifying suitable and reliable city-specific mitigation strategies from a wide range of green infrastructure solutions is inevitable, which should be done in the context of the regional climate of the area. Mesoscale modelling efforts are essential to fulfil that requirement in the pre-planning stages, and the importance of this stage remains overlooked. This specific resolution of 1 km is often used in the literature for much shorter experimental designs. This case study targets climate timescales (e.g., decades), and the spatial resolution of 1 km fits well with the objectives and requirements of this study. After identifying and specifying effective mitigation strategies for the selected area, urban planning should go beyond that by downscaling to microscale models into spatial layout perspective for all ecosystem services (which is not in the scope of this study). This study focused only on the summer. To achieve a complete understanding of the effectiveness of each surface parameter, a year-round assessment, including seasonal variations, is necessary. In addition, a cost-benefit analysis of each scenario would provide further support for decision-making.

5. Conclusion

This study investigated the effectiveness of combined urban surface parameters (natural and built) in mitigating seasonal average and excessive urban heat during summer in a temperate city, Melbourne, while considering operationalisability. Eighteen scenarios with different combinations of urban surface parameters, that is, urban trees (F1), green roofs (F2), and cool roofs (F3), were examined. The results demonstrate different levels of heat reduction benefits and limitations across the scenarios. Additionally, different scenarios proved effective for different heat indices. For example, higher ratios of cool roofs significantly reduced daytime temperatures, and vegetative surfaces promoted cooling at night.

Our results demonstrate the cooling ability of carefully planned urban surface parameters in a city. Most scenarios achieved reductions in heat indices, for example, seasonal averages, maximum and minimum temperatures, and extreme temperatures during heatwaves and UHI. The highest reduction was found for the scenario with maximum combined surface parameters, 20 % urban trees, 50 % green roofs, and cool roofs with a 0.7 albedo (S18) for multiple heat indices, such as average summer temperature (T_{ave}), minimum temperature (T_{min}), and urban heat island measured with the air temperature at 2 m above-ground (UHI). Another scenario, when the total roof area was converted to cool roofs of 0.7 albedo with 5 % increased urban trees (S12), could achieve the highest reduction for maximum summer temperature (T_{max}).

Implementing some strategies can be significantly more expensive than implementing others. The effectiveness of UGI should be defined based on both their thermal performance and operationalisability. Combined strategies seem to deliver the best diurnal thermal performance with practicality and cost. Our results showed that a combination of 20 % total urban trees, 50 % green roofs, and 50 % cool roofs with a 0.7 albedo (S18) had the highest effectiveness in Melbourne. Strategic planning with combined urban surfaces is more effective than adopting a single strategy for cities. Therefore, city planning should be strategically explored to achieve enhanced thermal benefits from a combination of urban surface parameters. Planting more trees in street canyons, establishing urban parks, and motivating urban residents for urban gardening are some of the methods to increase urban vegetation cover. Green and cool roofs can be promoted by encouraging investments and incentives for DIY and by changing and imposing regulations on construction for builders and developers. Establishing a UGI enhances the ecological value of a city while providing multiple ecosystem services. Therefore, these measures would enhance the diurnal thermal comfort of the city during heatwave events and ultimately promote liveability.

CRediT authorship contribution statement

Prabhasri Herath: Conceptualization, Methodology, Formal analysis, Investigation, Writing- Original Draft preparation, Editing and Visualization.

Marcus Thatcher: Conceptualization, Methodology, Software, Reviews & editing and Overall supervision.

Huidong Jin: Conceptualization, Methodology, Reviews & comments, and Overall supervision.

Xuemei Bai: Conceptualization, Methodology, Reviews & comments, Editing and Overall supervision.

Data availability

Data will be made available on request.

Declaration of competing interest

The authors declare that they have no known competing financial interests or personal relationships that could have appeared to influence the work reported in this paper.

Acknowledgement

The first author was funded by the Australian Government Research Training Program (AGRTP) Scholarship. The second and the third authors were partially supported by CSIRO Digiscape future science platform. We acknowledge NOAA PSL, Boulder, Colorado, USA, for providing NCEP/DOE Reanalysis II data (website: https://psl.noaa.gov).

Appendices. Supplementary data

Supplementary data to this article can be found online at https://doi.org/10.1016/j.scitotenv.2023.162476.

References

ABS, 2008. Water in Australia. Australia's Environments: Issues and Trends, 2007 by Australian Bureau of Statistics. Available: https://www.abs.gov.au/AUSSTATS/abs@.nsf/7d12b0f6763c78caca257061001cc588/330bc8fdfd50bee4ca2573c6001049f9!OpenDocument#:~:text=Water is a scarce resource in many parts of Australia&text=In recent years%2C low rainfall, further pressure on water supplies. (Accessed 30 October 2020).

AECOM, 2012. Economic Assessment of the Urban Heat Island Effect; Prepared for City of Melbourne. [Online]. Available:. https://www.melbourne.vic.gov.au/SiteCollectionDocuments/eco-assessment-of-urban-heat-island-effect.pdf.

Akbari, H., Konopacki, S., 2005. Calculating energy-saving potentials of heat-island reduction strategies. Energy Policy 33 (6), 721–756. https://doi.org/10.1016/j.enpol.2003.10.001.

Akbari, H., Menon, S., Rosenfeld, A., 2009. Global cooling: increasing world-wide urban albedos to offset CO2. Clim. Chang. 94 (3–4), 275–286. https://doi.org/10.1007/s10584-008-9515-9.

Ali, M., Iqbal, M.J., Sharif, M., 2013. Relationship between extreme temperature and electricity demand in Pakistan. Int. J. Energy Environ. Eng. 4 (1), 1–7. https://doi.org/10.1186/2251-6832-4-36.

Australian Energy Council, 2020. Solar Report, Quarter 3, 2019. [Online]. Available: https://www.energycouncil.com.au/media/7687/australian-energy-council-solar-report_march-2017.pdf.

Bai, X., 2018. Advance the ecosystem approach in cities. Nature 559 (7712), 7. https://doi.org/10.1038/d41586-018-05607-x Jul.

Barcelona City, Council, 2015. Guide to living terrace roofs and green roofs. In: Contreras, E., Castillo, I. (Eds.), Area of Urban Ecology. Barcelona City Council Available: https://bcnroc.ajuntament.barcelona.cat/jspui/handle/11703/98795.

Bherwani, H., Singh, A., Kumar, R., 2020. Assessment methods of urban microclimate and its parameters: a critical review to take the research from lab to land. Urban Clim. 34 (August), 100690. https://doi.org/10.1016/j.uclim.2020.100690.

BoM, 2016. How will I know if a heatwave is coming?. Available:Bureau of Meteorology http://media.bom.gov.au/social/blog/891/how-will-i-know-if-a-heatwave-is-coming/. (Accessed 20 July 2020)

BoM, 2020a. Climate statistics for Australian locations. (accessed Apr. 10, 2022). Available:Bureau of Meteorology http://www.bom.gov.au/climate/averages/tables/cw_086071.shtml.

BoM, 2020b. Annual climate statement 2019. (accessed Dec. 07, 2020). Available:Bureau of Meteorology http://www.bom.gov.au/climate/current/annual/aus/.

Bowler, D.E., Buyung-Ali, L., Knight, T.M., Pullin, A.S., 2010. Urban greening to cool towns and cities: a systematic review of the empirical evidence. Landsc. Urban Plan. 97 (3), 147–155. https://doi.org/10.1016/j.landurbplan.2010.05.006.

Bretz, S.E., Akbari, H., 1997. Long-term performance of high-albedo roof coatings. Energy Build. 25 (2), 159–167. https://doi.org/10.1016/s0378-7788(96)01005-5.

Broadbent, A.M., Declet-Barreto, J., Krayenhoff, E.S., Harlan, S.L., Georgescu, M., 2021. Targeted implementation of cool roofs for equitable urban adaptation to extreme heat. Sci. Total Environ. 811, 151326. https://doi.org/10.1016/j.scitotenv.2021.151326.

Brown, M.J., 2000. Urban parameterizations for mesoscale meteorological models. [Online]. Available:In: Boybeyi, Boybeyi (Eds.), Mesoscale Atmospheric Dispersion, no. January. WIT Press, Los Alamos, NM.

Chapman, S., Thatcher, M., Salazar, A., Watson, J.E.M., McAlpine, C.A., 2018. The effect of urban density and vegetation cover on the heat island of a subtropical city. J. Appl. Meteorol. Climatol. 57 (11), 2531–2550. https://doi.org/10.1175/JAMC-D-17-0316.1.

Chen, L., Liu, C., Zou, R., Yang, M., Zhang, Z., 2016. Experimental examination of effectiveness of vegetation as bio-filter of particulate matters in the urban environment. Environ. Pollut. 208, 198–208. https://doi.org/10.1016/j.envpol.2015.09.006.

Chen, X., Shuai, C., Chen, Z., Zhang, Y., 2019. What are the root causes hindering the implementation of green roofs in urban China? Sci. Total Environ. 654, 742–750. https://doi.org/10.1016/j.scitotenv.2018.11.051.

City of Melbourne, 2012. Urban Forest Strategy: making a great city greener 2012-2032. [Online]. Available: https://www.melbourne.vic.gov.au/Sustainability/UrbanForest/Documents/Urban_Forest_Strategy.pdf.

City of Melbourne, 2014. Cool Roofs: A City of Melbourne Guide. [Online]. Available:. https://www.melbourne.vic.gov.au/SiteCollectionDocuments/cool-roofs-guide.pdf.

City of Melbourne, 2016. 1200 BUILDINGS: Advice Sheet. [Online]. Available: http://www.melbourne.vic.gov.au/SiteCollectionDocuments/1200-buildings-advice.PDF.

City of Melbourne, 2017. Green our city, Strategic action plan 2017 - 2021. [Online]. Available: https://www.melbourne.vic.gov.au/sitecollectiondocuments/green-our-city-action-plan-2018.pdf.

Coutts, A.M., Beringer, J., Tapper, N.J., 2007. Impact of increasing urban density on local climate: spatial and temporal variations in the surface energy balance in Melbourne, Australia. J. Appl. Meteorol. Climatol. 46 (4), 477–493. https://doi.org/10.1175/JAM2462.1.

Coutts, A.M., Beringer, J., Tapper, N.J., 2008. Investigating the climatic impact of urban planning strategies through the use of regional climate modelling: a case study for Melbourne, Australia. Int. J. Climatol. 28 (March 2008), 2011–2029. https://doi.org/10.1002/joc.1680.

Cowan, T., Purich, A., Perkins, S., Pezza, A., Boschat, G., Sadler, K., 2014. More frequent, longer, and hotter heat waves for Australia in the twenty-first century. J. Clim. 27 (15), 5851–5871. https://doi.org/10.1175/JCLI-D-14-00092.1.

DEA, 2020. Heatwaves and Health in Australia: Fact Sheet. [Online]. Available:. http://dea.org.au/resources/file/climate-change-and-health-in-australia.

DEPI, 2014. A Guide to Green Roofs, Walls and Facades. Department of Environment and Primary Industries, Melbourne, Australia.

Dey, R., Lewis, S.C., Arblaster, J.M., Abram, N.J., 2019. A review of past and projected changes in Australia's rainfall. Wiley Interdiscip. Rev. Clim. Chang. 10 (3), 1–23. https://doi.org/10.1002/wcc.577.

Di Giuseppe, E., D'Orazio, M., 2014. Assessment of the effectiveness of cool and green roofs for the mitigation of the Heat Island effect and for the improvement of thermal comfort in nearly zero energy building. Archit. Sci. Rev. 58 (2), 134–143. https://doi.org/10.1080/00038628.2014.966050.

Downton, P., 2013. Green roofs and walls. Your Home: Australia's guide to environmentally sustainable homes. Available: https://www.yourhome.gov.au/materials/green-roofs-and-walls. (Accessed 22 September 2021).

Environmental Protection Agency, 2011. Urban Heat Island Basics. [Online]. Available:. https://www.epa.gov/sites/default/files/2014-06/documents/basicscompendium.pdf.

Fischer, E.M., Oleson, K.W., Lawrence, D.M., 2012. Contrasting urban and rural heat stress responses to climate change. Geophys. Res. Lett. 39 (3), 1–8. https://doi.org/10.1029/2011GL050576.

Fowdar, H.S., Hatt, B.E., Breen, P., Cook, P.L.M., Deletic, A., 2017. Designing living walls for greywater treatment. Water Res. 110, 218–232. https://doi.org/10.1016/j.watres.2016.12.018.

Gibson, C., 2021. How to create a green roof in Australia. Available: https://hipages.com.au/article/green_roofs. (Accessed 22 September 2021).

Giyasova, I., 2021. Factors affecting microclimatic conditions in urban environment. E3S Web Conf. 244, 1–7. https://doi.org/10.1051/e3sconf/202124406010.

Grard, B.J.P., Chenu, C., Manouchehri, N., Houot, S., Frascaria-Lacoste, N., Aubry, C., 2018. Rooftop farming on urban waste provides many ecosystem services. Agron. Sustain. Dev. 38 (1), pp. https://doi.org/10.1007/s13593-017-0474-2.

Grimmond, S., 2007. Urbanization and global environmental change: local effects of urban warming. Geogr. J. 173 (1), 83–88. https://doi.org/10.1111/j.1475-4959.2007.232_3.x.

Gul, M., Kotak, Y., Muneer, T., Ivanova, S., 2018. Enhancement of Albedo for solar energy gain with particular emphasis on overcast skies. Energies 11 (11), 1–17. https://doi.org/10.3390/en11112881.

Gunawardena, K.R., Wells, M.J., Kershaw, T., 2017. Utilising green and bluespace to mitigate urban heat island intensity. Sci. Total Environ. 584–585, 1040–1055. https://doi.org/10.1016/j.scitotenv.2017.01.158.

Gupta, N., Mathew, A., Khandelwal, S., 2019. Analysis of cooling effect of water bodies on land surface temperature in nearby region: a case study of Ahmedabad and Chandigarh cities in India. Egypt. J. Remote Sens. Sp. Sci. 22 (1), 81–93. https://doi.org/10.1016/j.ejrs.2018.03.007.

Harman, I.N., Best, M.J., Belcher, S.E., 2004. Radiative exchange in an urban street canyon. Bound.-Layer Meteorol. 110 (2), 301–316. https://doi.org/10.1023/A:1026029822517.

Herath, H.M.P.I.K., Halwatura, R.U., Jayasinghe, G.Y., 2018. Evaluation of green infrastructure effects on tropical Sri Lankan urban context as an urban heat island adaptation strategy. Urban For. Urban Green. 29. https://doi.org/10.1016/j.ufug.2017.11.013.

Herath, P., Halwatura, R.U., Jayasinghe, G.Y., 2018. Modeling a tropical urban context with green walls and green roofs as an urban heat island adaptation strategy. Procedia Eng. 212. https://doi.org/10.1016/j.proeng.2018.01.089.

Herath, P., Thatcher, M., Jin, H., Bai, X., 2021. Effectiveness of urban surface characteristics as mitigation strategies for the excessive summer heat in cities. Sustain. Cities Soc. 72 (June), 103072. https://doi.org/10.1016/j.scs.2021.103072.

Heusinger, J., Sailor, D.J., Weber, S., 2018. Modeling the reduction of urban excess heat by green roofs with respect to different irrigation scenarios. Build. Environ. 131 (October 2017), 174–183. https://doi.org/10.1016/j.buildenv.2018.01.003.

Hou, Y.L., Mu, H.Z., Dong, G.T., Shi, J., 2014. Influences of urban temperature on the electricity consumption of Shanghai. Adv. Clim. Chang. Res. 5 (2), 74–80. https://doi.org/10.3724/SP.J.1248.2014.074.

O'Donoghue, J., 2016. A guide for specifying green roofs in Australia. Architecture & Design. Available: https://www.architectureanddesign.com.au/features/features-articles/a-guide-for-specifying-green-roofsin-australia#.

Hurley, P., 2008a. TAPM V4. User Manual, No. 5. CSIRO Marine and Atmospheric Research Internal Report No. 5 (October 2008). , pp. 1–35 ISBN: 978-1-921424-73-1. Available: https://www.cmar.csiro.au/research/tapm/docs/tapm_v4_user_manual.pdf.

Hurley, P.J., 2008b. TAPM V4. Part 1: Technical Description, no. 25. CSIRO Marine and Atmospheric Research paper No. 25 (October 2008). , pp. 1–59 ISBN: 978-1-921424-71-7. Available: https://www.cmar.csiro.au.

Imran, H.M., Kala, J., Ng, A.W.M., Muthukumaran, S., 2018. Effectiveness of green and cool roofs in mitigating urban heat island effects during a heatwave event in the city of

Melbourne in southeast Australia. J. Clean. Prod. 197, 393–405. https://doi.org/10.1016/j.jclepro.2018.06.179.
Imran, H.M., Kala, J., Ng, A.W.M., Muthukumaran, S., 2019. Effectiveness of vegetated patches as green infrastructure in mitigating Urban Heat Island effects during a heatwave event in the city of Melbourne. Weather Clim. Extrem. 25 (June). https://doi.org/10.1016/j.wace.2019.100217.
Imran, H.M., Kala, J., Ng, A.W.M., Muthukumaran, S., 2019. Impacts of future urban expansion on urban heat island effects during heatwave events in the city of Melbourne in southeast Australia. Q. J. R. Meteorol. Soc. 145 (723), 2586–2602. https://doi.org/10.1002/qj.3580.
Jacobs, S.J., Gallant, A.J.E., Tapper, N.J., Li, D., 2018. Use of cool roofs and vegetation to mitigate urban heat and improve human thermal stress in Melbourne, Australia. J. Appl. Meteorol. Climatol. 57 (8), 1747–1764. https://doi.org/10.1175/JAMC-D-17-0243.1.
Jacobs, C., Klok, L., Bruse, M., Cortesão, J., Lenzholzer, S., Kluck, J., 2020. Are urban water bodies really cooling? Urban Clim. 32 (January), 100607. https://doi.org/10.1016/j.uclim.2020.100607.
Jamei, E., Chau, H.W., Seyedmahmoudian, M., Stojcevski, A., 2021. Review on the cooling potential of green roofs in different climates. Sci. Total Environ. 791, 148407. https://doi.org/10.1016/j.scitotenv.2021.148407.
Jiao, M., Zhou, W., Zheng, Z., Wang, J., Qian, Y., 2017. Patch size of trees affects its cooling effectiveness: a perspective from shading and transpiration processes. Agric. For. Meteorol. 247 (August), 293–299. https://doi.org/10.1016/j.agrformet.2017.08.013.
Joshi, M.Y., Selmi, W., Binard, M., Nys, G.A., Teller, J., 2020. Potential for urban greening with green roofs: a way towards smart cities. ISPRS Ann. Photogramm. Remote Sens. Spat. Inf. Sci. vol. 6, no. 4/W2, pp. 87–94. https://doi.org/10.5194/isprs-annals-VI-4-W2-2020-87-2020.
Kanamitsu, M., et al., 2002. NCEP–DOE AMIP-II reanalysis (R-2). Bull. Am. Meteorol. Soc. 83 (11), 1631–1644. https://doi.org/10.1175/BAMS-83-11.
Kowalczyk, E.A., Garratt, J.R., Krummel, P.B., 1994. Implementation of a soil-canopy scheme into the CSIRO GCM: regional aspects of the model response. [Online]. Available:CSIRO Div. Atmos. Res. Tech. Pap. no. 32. vol. 32 , pp. 1–65.. http://www.csa.com/partners/viewrecord.php?requester=gs&collection=TRD&recid=N9524192AH.
Krayenhoff, E.S., Voogt, J.A., 2010. Impacts of urban albedo increase on local air temperature at daily-annual time scales: model results and synthesis of previous work. J. Appl. Meteorol. Climatol. 49 (8), 1634–1648. https://doi.org/10.1175/2010JAMC2356.1.
Krayenhoff, E.S., et al., 2020. A multi-layer urban canopy meteorological model with trees (BEP-Tree): street tree impacts on pedestrian-level climate. Urban Clim. 32 (July 2019), 100590. https://doi.org/10.1016/j.uclim.2020.100590.
Krayenhoff, E.S., et al., 2021. Cooling hot cities: a systematic and critical review of the numerical modelling literature. Environ. Res. Lett. 16 (5). https://doi.org/10.1088/1748-9326/abdcf1.
Kueh, M.T., Lin, C.Y., Chuang, Y.J., Sheng, Y.F., Chien, Y.Y., 2017. Climate variability of heat waves and their associated diurnal temperature range variations in Taiwan. Environ. Res. Lett. 12 (7). https://doi.org/10.1088/1748-9326/aa70d9.
Larsen, M.A.D., Thejll, P., Christensen, J.H., Refsgaard, J.C., Jensen, K.H., 2013. On the role of domain size and resolution in the simulations with the HIRHAM region climate model. Clim. Dyn. 40 (11–12), 2903–2918. https://doi.org/10.1007/s00382-012-1513-y.
Li, D., Bou-Zeid, E., 2013. Synergistic interactions between urban heat islands and heat waves: the impact in cities is larger than the sum of its parts. J. Appl. Meteorol. Climatol. 52 (9), 2051–2064. https://doi.org/10.1175/JAMC-D-13-02.1.
Li, X.X., Norford, L.K., 2016. Evaluation of cool roof and vegetations in mitigating urban heat island in a tropical city, Singapore. Urban Clim. 16, 59–74. https://doi.org/10.1016/j.uclim.2015.12.002.
Li, W.C., Yeung, K.K.A., 2014. A comprehensive study of green roof performance from environmental perspective. Int. J. Sustain. Built Environ. 3 (1), 127–134. https://doi.org/10.1016/j.ijsbe.2014.05.001.
Li, D., Bou-Zeid, E., Oppenheimer, M., 2014. The effectiveness of cool and green roofs as urban heat island mitigation strategies. Environ. Res. Lett. 9 (5). https://doi.org/10.1088/1748-9326/9/5/055002.
Li, D., et al., 2019. Urban heat island: aerodynamics or imperviousness? Sci. Adv. 5 (4), 1–5. https://doi.org/10.1126/sciadv.aau4299.
Li, Y., Schubert, S., Kropp, J.P., Rybski, D., 2020. On the influence of density and morphology on the Urban Heat Island intensity. Nat. Commun. 11 (1), 1–9. https://doi.org/10.1038/s41467-020-16461-9.
Lin, B.S., Yu, C.C., Su, A.T., Lin, Y.J., 2013. Impact of climatic conditions on the thermal effectiveness of an extensive green roof. Build. Environ. 67, 26–33. https://doi.org/10.1016/j.buildenv.2013.04.026.
Lindfield, M., Teipelke, R., 2017. How to finance urban infrastructure - Explainer. [Online]. Available: https://www.c40cff.org/knowledge-library/explainer-how-to-finance-urban-infrastructure.
Lipson, M.J., Thatcher, M., Hart, M.A., Pitman, A., 2018. A building energy demand and urban land surface model. Q. J. R. Meteorol. Soc. 144 (714), 1572–1590. https://doi.org/10.1002/qj.3317.
Longden, T., Quilty, S., Haywood, P., Hunter, A., Gruen, R., 2020. Heat-related mortality: an urgent need to recognise and record. Lancet Planet. Health 4 (5), e171. https://doi.org/10.1016/S2542-5196(20)30100-5.
Macintyre, H.L., Heaviside, C., Cai, X., Phalkey, R., 2021. Comparing temperature-related mortality impacts of cool roofs in winter and summer in a highly urbanized European region for present and future climate. Environ. Int. 154 (May), 106606. https://doi.org/10.1016/j.envint.2021.106606.
Martilli, A., Krayenhoff, E.S., Nazarian, N., 2020. Is the Urban Heat Island intensity relevant for heat mitigation studies? Urban Clim. 31 (September 2019), 1–4. https://doi.org/10.1016/j.uclim.2019.100541.
Masoudi, M., Tan, P.Y., Liew, S.C., 2019. Multi-city comparison of the relationships between spatial pattern and cooling effect of urban green spaces in four major Asian cities. Ecol. Indic. 98 (November 2018), 200–213. https://doi.org/10.1016/j.ecolind.2018.09.058.
Mcpherson, E.G., 1994. Cooling urban heat islands with sustainable landscapes. In: Rutherford, P.H., Rowntree, R.A., Muick, P.C. (Eds.), The Ecological City: Preserving and Restoring Urban Biodiversity. University of Massachusetts Press, Amherst, MA, pp. 151–171.
Meili, N., et al., 2021. Tree effects on urban microclimate: diurnal, seasonal, and climatic temperature differences explained by separating radiation, evapotranspiration, and roughness effects. Urban For. Urban Green. 58, 126970. https://doi.org/10.1016/j.ufug.2020.126970.
Morini, E., Touchaei, A.G., Rossi, F., Cotana, F., Akbari, H., 2018. Evaluation of Albedo enhancement to mitigate impacts of urban heat island in Rome (Italy) using WRF meteorological model. Urban Clim. 24 (August), 551–566. https://doi.org/10.1016/j.uclim.2017.08.001.
Morris, C.J.G., Simmonds, I., Plummer, N., 2001. Quantification of the influence of wind and cloud on the nocturnal urban heat island of a large city. J. Appl. Meteorol. 40 (2), 169–182. https://doi.org/10.1175/1520-0450(2001)040<0169:QOTIOW>2.0.CO;2.
Oke, T.R., 1988. The urban energy balance. Prog. Phys. Geogr. 12 (4), 471–508. https://doi.org/10.1177/030913338801200401.
Oke, T.R., Johnson, G.T., Steyn, D.G., Watson, I.D., 1991. Simulation of surface urban heat islands under 'ideal' conditions at night part 2: diagnosis of causation. Bound.-Layer Meteorol. 56 (4), 339–358. https://doi.org/10.1007/BF00119211.
Onori, A., Lavau, S., Fletcher, T., 2018. Implementation as more than installation: a case study of the challenges in implementing green infrastructure projects in two Australian primary schools. Urban Water J. 15 (9), 911–917. https://doi.org/10.1080/1573062X.2019.1574842.
Osmond, P., Sharifi, E., Hatvani-Kovacs, G., Bush, J., Fox, J., 2017. Guide to Urban Cooling Strategies. [Online]. Available:. http://www.lowcarbonlivingcrc.com.au/resources/crc-publications/crclcl-project-reports/guide-urban-cooling-strategies.
Oswald, S.M., et al., 2020. Using urban climate modelling and improved land use classifications to support climate change adaptation in urban environments: a case study for the city of Klagenfurt, Austria. Urban Clim. 31 (July 2019), 100582. https://doi.org/10.1016/j.uclim.2020.100582.
Papangelis, G., Tombrou, M., Dandou, A., Kontos, T., 2012. An urban 'green planning' approach utilizing the Weather Research and Forecasting (WRF) modeling system. A case study of Athens, Greece. Landsc. Urban Plan. 105 (1–2), 174–183. https://doi.org/10.1016/j.landurbplan.2011.12.014.
Park, C.Y., et al., 2019. Variations in pedestrian mean radiant temperature based on the spacing and size of street trees. Sustain. Cities Soc. 48 (March), 1–9. https://doi.org/10.1016/j.scs.2019.101521.
Patricola, C.M., Wehner, M.F., 2018. Anthropogenic influences on major tropical cyclone events. Nature 563 (7731), 339–346. https://doi.org/10.1038/s41586-018-0673-2.
Perkins, S.E., 2015. A review on the scientific understanding of heatwaves-their measurement, driving mechanisms, and changes at the global scale. Atmos. Res. 164–165, 242–267. https://doi.org/10.1016/j.atmosres.2015.05.014.
Perkins-Kirkpatrick, S.E., et al., 2016. Natural hazards in Australia: heatwaves. Clim. Chang. 139 (1), 101–114. https://doi.org/10.1007/s10584-016-1650-0.
Phillips, N., 2020. Climate change made Australia's devastating fire season 30% more likely. Nature https://doi.org/10.1038/d41586-020-00627-y no. Advance online publication.
Prodanovic, V., Hatt, B., McCarthy, D., Zhang, K., Deletic, A., 2017. Green walls for greywater reuse: understanding the role of media on pollutant removal. Ecol. Eng. 102, 625–635. https://doi.org/10.1016/j.ecoleng.2017.02.045.
Pugh, T.A.M., MacKenzie, A.R., Whyatt, J.D., Hewitt, C.N., 2012. Effectiveness of green infrastructure for improvement of air quality in urban street canyons. Environ. Sci. Technol. 46 (14), 7692–7699. https://doi.org/10.1021/es300826w.
Reimer, M., Rusche, K., 2019. Green infrastructure under pressure. A global narrative between regional vision and local implementation. Eur. Plan. Stud. 27 (8), 1542–1563. https://doi.org/10.1080/09654313.2019.1591346.
Richards, D.R., Fung, T.K., Belcher, R.N., Edwards, P.J., 2019. Differential air temperature cooling performance of urban vegetation types in the tropics. Urban For. Urban Green. 50 (June), 2020. https://doi.org/10.1016/j.ufug.2020.126651.
Rogers, A., 2018. Cities Grab Onto Hurricanes; Buildings Make the Rain Worse. Available: Wired https://www.wired.com/story/cities-cause-hurricanes-to-dump-extra-rain-on-them/. (Accessed 7 December 2020).
Roth, M., 2013. Urban heat islands. In: Fernando, H.J.S. (Ed.), Environmental Indicators. CRC Press/Taylor & Francis Group, LLC, pp. 67–75.
Santamouris, M., Synnefa, A., Karlessi, T., 2011. Using advanced cool materials in the urban built environment to mitigate heat islands and improve thermal comfort conditions. Sol. Energy 85 (12), 3085–3102. https://doi.org/10.1016/j.solener.2010.12.023.
Schiermeier, Q., 2019. Europe's mega-heatwave boosted by climate change. Nat. Focus News 571, 155.
Schiermeier, Q., 2021. Climate change made North America's deadly heatwave 150 times more likely. Nature https://doi.org/10.1038/d41586-021-01869-0 no. Advance online publication.
Sharma, A., Conry, P., Fernando, H.J.S., Hamlet, A.F., Hellmann, J.J., Chen, F., 2016. Green and cool roofs to mitigate urban heat island effects in the Chicago metropolitan area: evaluation with a regional climate model. Environ. Res. Lett. 11 (6). https://doi.org/10.1088/1748-9326/11/6/064004.
Shi, P., et al., 2017. Urbanization and air quality as major drivers of altered spatiotemporal patterns of heavy rainfall in China. Landsc. Ecol. 32 (8), 1723–1738. https://doi.org/10.1007/s10980-017-0538-3.
Stewart, I.D., Oke, T.R., 2012. Local climate zones for urban temperature studies. Bull. Am. Meteorol. Soc. 93 (12), 1879–1900. https://doi.org/10.1175/BAMS-D-11-00019.1.
Sun, C., et al., 2019. Urban Vegetation, Urban Heat Islands and Heat Vulnerability Assessment in Melbourne, 2018. [Online]. Available:. https://www.planning.vic.gov.au/__data/assets/pdf_file/0018/440181/UHI-and-HVI2018_Report_v1.pdf.
Taha, H., 1997. Urban climates and heat islands: Albedo, evapotranspiration, and anthropogenic heat. Energy Build. 25 (96), 99–103. https://doi.org/10.1016/S0378-7788(96)00999-1.

Thatcher, M., Hurley, P., 2012. Simulating Australian urban climate in a mesoscale atmospheric numerical model. Bound.-Layer Meteorol. 142 (1), 149–175. https://doi.org/10.1007/s10546-011-9663-8.

Theeuwes, N.E., Solcerová, A., Steeneveld, G.J., 2013. Modeling the influence of open water surfaces on the summertime temperature and thermal comfort in the city. J. Geophys. Res. Atmos. 118 (16), 8881–8896. https://doi.org/10.1002/jgrd.50704.

Tong, Z., Whitlow, T.H., Landers, A., Flanner, B., 2016. A case study of air quality above an urban roof top vegetable farm. Environ. Pollut. 208, 256–260. https://doi.org/10.1016/j.envpol.2015.07.006.

Uni.Melbourne, 2011. Cool Roofs: City of Melbourne Research Report. [Online]. Available:. https://www.melbourne.vic.gov.au/sitecollectiondocuments/cool-roofs-report.pdf.

VAGO, 2014. Heatwave Management: Reducing the Risk to Public Health. Available: Victorian Auditor-General's Office https://www.audit.vic.gov.au/report/heatwave-management-reducing-risk-public-health. (Accessed 21 June 2022).

Victoria State Government, 2017. Plan Melbourne 2017-2050 a Global City of Opportunity and Choice.

Viecco, M., et al., 2018. Potential of particle matter dry deposition on green roofs and living walls vegetation for mitigating urban atmospheric pollution in semiarid climates. <sb:maintitle>Sustainability</sb:maintitle> 10 (7). https://doi.org/10.3390/su10072431.

Wang, Z.H., Zhao, X., Yang, J., Song, J., 2016. Cooling and energy saving potentials of shade trees and urban lawns in a desert city. Appl. Energy 161, 437–444. https://doi.org/10.1016/j.apenergy.2015.10.047.

Wever, N., 2012. Quantifying trends in surface roughness and the effect on surface wind speed observations. J. Geophys. Res. Atmos. 117 (11), 1–14. https://doi.org/10.1029/2011JD017118.

WHO, 2018a. Heat and Health. Fact sheets (accessed Jun. 30, 2020). Available:Newsroom https://www.who.int/news-room/fact-sheets/detail/climate-change-heat-and-health.

WHO, 2018b. Heatwaves. Available: https://www.who.int/health-topics/heatwaves#tab=tab_1. (Accessed 10 July 2020).

Wilkinson, S., Brown, P., Ghosh, S., 2017. Expanding the Living Architecture in Australia. Hort Innovation, Sydney, Australia.

Williams, S., et al., 2012. Heat and health in Adelaide, South Australia: assessment of heat thresholds and temperature relationships. Sci. Total Environ. 414, 126–133. https://doi.org/10.1016/j.scitotenv.2011.11.038.

Wondmagegn, B.Y., et al., 2021. Impact of heatwave intensity using excess heat factor on emergency department presentations and related healthcare costs in Adelaide, South Australia. Sci. Total Environ. 781, 146815. https://doi.org/10.1016/j.scitotenv.2021.146815.

Wonorahardjo, S., et al., 2020. Characterising thermal behaviour of buildings and its effect on urban heat island in tropical areas. Int. J. Energy Environ. Eng. 11 (1), 129–142. https://doi.org/10.1007/s40095-019-00317-0.

Xing, Y., Jones, P., 2019. In-situ monitoring of energetic and hydrological performance of a semi-intensive green roof and a white roof during a heatwave event in the UK. Indoor Built Environ., 1–14 https://doi.org/10.1177/1420326X19887218.

Yenneti, K., 2020. After another hot summer, here are 6 ways to cool our cities in future. Available:The Conversation https://theconversation.com/after-another-hot-summer-here-are-6-ways-to-cool-our-cities-in-future-110817. (Accessed 2 December 2020).

Yenneti, K., Santamouris, M., Prasad, D., Ding, L., 2017. Cooling Cities- Strategies and Technologies to Mitigate Urban Heat- Discussion Paper. [Online]. Available:. https://www.preventionweb.net/publications/view/54493.

Young, T.M., Cameron, D.D., Phoenix, G.K., 2017. Increasing green roof plant drought tolerance through substrate modification and the use of water retention gels. Urban Water J. 14 (6), 551–560. https://doi.org/10.1080/1573062X.2015.1036761.

Zeder, L., 2015. How to heat-proof our cities for the future. EngineeringJobs.com.au. (Accessed 2 December 2020) Available: https://www.engineerjobs.com.au/article/how-to-heat-proof-our-cities-for-the-future/586.

Zhang, W., Villarini, G., Vecchi, G.A., Smith, J.A., 2018. Urbanization exacerbated the rainfall and flooding caused by hurricane Harvey in Houston. Nature 563 (7731), 384–388. https://doi.org/10.1038/s41586-018-0676-z.

Zhao, L., Lee, X., Smith, R.B., Oleson, K., 2014. Strong contributions of local background climate to urban heat islands. Nature 511 (7508), 216–219. https://doi.org/10.1038/nature13462.

Zhou, B., Rybski, D., Kropp, J.P., 2017. The role of city size and urban form in the surface urban heat island. Sci. Rep. 7 (1), 1–9. https://doi.org/10.1038/s41598-017-04242-2.

Zinzi, M., Agnoli, S., 2012. Cool and green roofs. An energy and comfort comparison between passive cooling and mitigation urban heat island techniques for residential buildings in the Mediterranean region. Energy Build. 55, 66–76. https://doi.org/10.1016/j.enbuild.2011.09.024.

Zuniga-Teran, A.A., et al., 2020. Challenges of mainstreaming green infrastructure in built environment professions. J. Environ. Plan. Manag. 63 (4), 710–732. https://doi.org/10.1080/09640568.2019.1605890.